Table 1
Clinical diagnosis of transfusion-related adverse events from 2007 to 2010.

	RBC cases (%)	FFP cases (%)	PC cases (%)
Non-haemolytic transfusion reaction			
Severe allergic reaction	4 (0.5%)	7 (1.3%)	8 (0.4%)
TRALI	4 (0.5%)	3 (0.6%)	3 (0.1%)
TACO	4 (0.5%)	1 (0.2%)	0
PTP	0	0	0
GVHD	0	0	0
Others	861 (97.7%)	509 (97.9%)	2127 (99.5%)
Haemolytic transfusion reaction			
Acute hemolytic reaction	3 (0.3%)	0	0
Delayed hemolytic reaction	1 (0.1%)	0	0
Infectious diseases			
HBV	1 (0.1%)	0	0
HCV	0	0	0
HIV	0	0	0
Bacteria	0	0	0
Others	0	0	0
Total all cases	881	520	2138

The number of events and their frequency for each blood component are shown. TRALI, transfusion-related acute lung injury; TACO, transfusion associated circulatory overload; PTP, transfusion purpura; GVHD, graft-versus-host disease; HBV, hepatitis B virus; HCV, hepatitis C virus; HIV, human immunodeficiency virus.

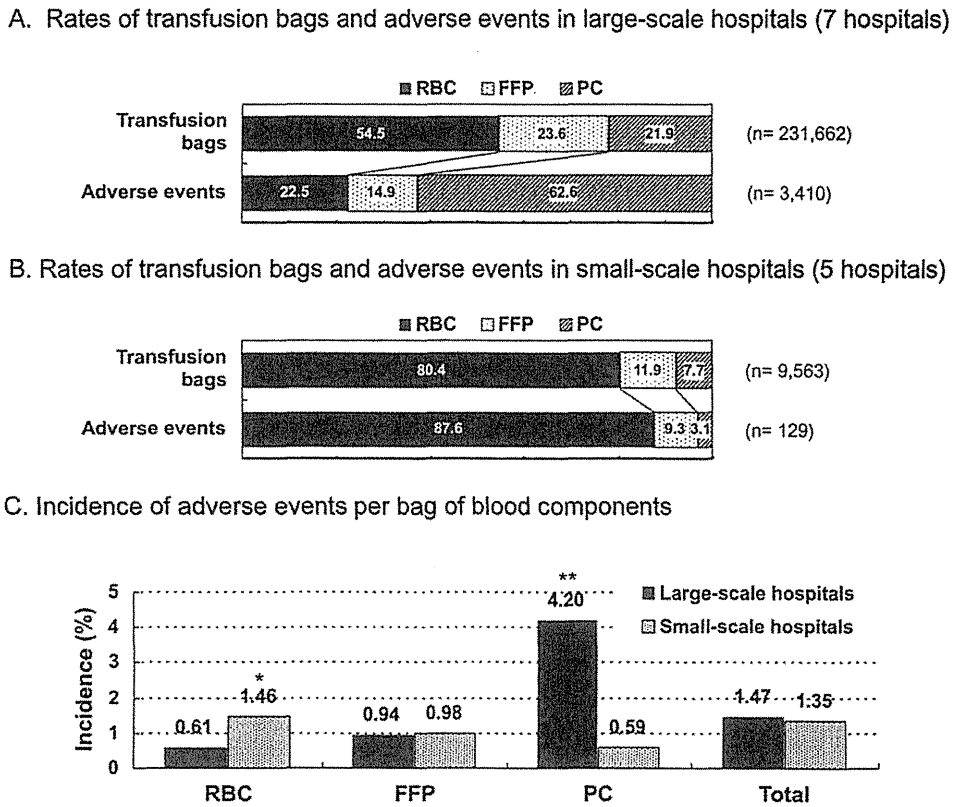

Fig. 6. Comparison of use of transfusion bag type, adverse events and incidence between large-scale and small-scale hospitals. Proportions of type of blood component and adverse events by type of blood component in seven large-scale university hospitals (A) and in five small-scale hospitals (fewer than 300 beds) (B). (C) The incidence of adverse events per bag of each blood component in large-scale and small-scale hospitals. $^{*}p < 0.05$ compared with large-scale hospitals; $^{**}p < 0.01$ compared with small-scale hospitals.

5. Conclusions

We have developed a comprehensive online system for the collection of all adverse reactions in recipients related to blood transfusion. Despite the limitation of our current system described above, this system is effective for collection and analysis of actual adverse events in recipients and can be used to enhance the existing surveillance system in Japan.

Conflict of interest statement

The authors declare no competing financial interests.

Acknowledgments

This study was supported by a Grant from the Ministry of Health, Labour and Welfare of Japan and by The Japan Society of Transfusion Medicine and Cell Therapy.

References

[1] de Vries RRP, Faber JC, Strengers PFW. Members of the board of the international haemovigilance network. Haemovigilance: an effective tool for improving transfusion practice. Vox Sang 2011;100:60–7.
[2] Carlier M, Vo Mai MP, Fauveau L, Ounnoughene N, Sandid I, Renaudier P. Seventeen years of haemovigilance in France: assessment and outlook. Transfus Clin Biol 2011;18:140–50.
[3] Keller-Stanislawski B, Lohmann A, Günay S, Heiden M, Funk MB. The German haemovigilance system–reports of serious adverse transfusion reactions between 1997 and 2007. Transfus Med 2009;19:340–9.
[4] Strengers PF. Is haemovigilance improving transfusion practice? The European experience. Dev Biol (Basel) 2007;127:215–24.
[5] Giampaolo A, Piccinini V, Catalano L, Abbonizio F, Hassan HJ. The first data from the haemovigilance system in Italy. Blood Transfus 2007;5:66–74.
[6] Stainsby D, Jones H, Asher D, Atterbury C, Boncinelli A, Brant L, et al. SHOT steering group. Serious hazards of transfusion: a decade of hemovigilance in the UK. Transfus Med Rev 2006;20:273–82.
[7] Okazaki H. The benefits of the Japanese haemovigilance system for better patient care. Vox Sang. 2007;2:104–9.
[8] Robillard P. The ISBT working party on haemovigilance. Transfus. Today 2006;68:4–7.
[9] Andreu G, Morel P, Forestier F, Debeir J, Rebibo D, Janvier G, et al. Hemovigilance network in France. organization and analysis of immediate transfusion incident reports from 1994 to 1998. Transfusion 2002;42:1356–64.
[10] Rouger P, Noizat-Pirenne F, Le Pennec PY. Haemovigilance and transfusion safety in France. Vox Sang. 2000;78:287–9.
[11] Michlig C, Vu DH, Wasserfallen JB, Spahn DR, Schneider P, Tissot JD. Three years of haemovigilance in a general university hospital. Transfus. Med. 2003;13:63–73.
[12] Siegenthaler MA, Schneider P, Vu DH, Tissot JD. Haemovigilance in a general university hospital: need for a more comprehensive classification and a codification of transfusion-related events. Vox Sang. 2005;88:22–30.

Journal of Bioscience and Bioengineering
VOL. 115 No. 1, 104–110, 2013

ELSEVIER

www.elsevier.com/locate/jbiosc

Aggregation analysis of pharmaceutical human immunoglobulin preparations using size-exclusion chromatography and analytical ultracentrifugation sedimentation velocity

Elena Krayukhina,[1] Susumu Uchiyama,[1] Kiyoko Nojima,[2] Yoshiaki Okada,[2] Isao Hamaguchi,[2] and Kiichi Fukui[1,*]

Graduate School of Engineering, Osaka University, 2-1 Yamadaoka, Suita 565-0871, Japan[1] and Department of Safety Research on Blood and Biological Products, National Institute of Infectious Diseases, 4-7-1 Gakuen Musashi-Murayama-shi, Tokyo 208-0011, Japan[2]

Received 27 June 2012; accepted 31 July 2012
Available online 24 August 2012

In the pharmaceutical industry, analysis of soluble aggregates in pharmaceutical formulations is most commonly performed using size-exclusion chromatography (SEC). However, owing to concerns that aggregates can be overlooked by SEC analysis, it has been suggested that its results should be confirmed with orthogonal methods. One of the main alternative methods for SEC is analytical ultracentrifugation sedimentation velocity (AUC-SV), which has been indicated as an important tool for the measurement of protein aggregation. The present study aimed to show that AUC-SV can be effectively applied for the characterization of marketed immunoglobulin pharmaceutical preparations to support the results obtained by SEC. In addition, the present research aimed to assess the appropriateness of two integration approaches for the quantitative analysis of the SEC results. Thus, the aggregates were measured in seven different preparations of human immunoglobulins by AUC-SV and SEC, and the acquired chromatographic data were processed by using either the vertical drop method or the Gaussian skim approach, implemented in the Empower II chromatography data software (Waters, Tokyo, Japan). The results of aggregation measurements performed using AUC-SV were in good agreement with those obtained using SEC. As expected, the Gaussian skim integration approach inherently provided lower estimates of aggregation content than the results of the vertical drop method. The finding of this study confirmed the complementary nature of AUC-SV to SEC for aggregate composition analysis and underscored the important role that the different integration methods can play in the quantitative interpretation of chromatographic results.

[**Key words:** Immunoglobulin; Size-exclusion chromatography; Vertical drop method; Gaussian skim; Analytical ultracentrifugation sedimentation velocity]

Antibody aggregation is a common problem in the pharmaceutical industry, encountered during the manufacturing process and long-term storage of antibody products. It was suggested that the presence of antibody aggregates in a therapeutic product can affect drug efficacy or may even cause immunogenic reactions when administered to patients (1). To ensure that the biotherapeutic product is consistent with quality standards and meets all regulatory requirements, an accurate measurement of aggregation content is necessary.

Size-exclusion chromatography (SEC) is currently employed for the quantification of soluble antibody aggregates as a quality control method. SEC separates molecules based on their hydrodynamic volume, provides highly reproducible results, is easy to perform, and is a relatively fast technique for the characterization of pharmaceutical formulations. The elution profiles generated by SEC are analyzed, and the fractional amount of each solute detected in the sample is estimated from the area under the peak, which is calculated using chromatographic software. In general, the area under unresolved peaks is determined by the vertical drop method. This method involves the addition of a vertical line from the valley between the peaks to the horizontal baseline. However, the perpendicular separation of overlapping peaks has previously been shown to introduce significant errors in peak area estimation (2–4). Alternative approaches implemented in chromatographic data analysis packages allow more sophisticated approaches for the identification of unresolved peaks, such as the Gaussian skim method implemented in the Empower II software. This algorithm fits the shapes of the peaks observed in the chromatogram using a Gaussian profile and is assumed to better represent the shape of the parent peak in the overlapping peaks group. Nevertheless, the vertical drop method remains the most commonly applied approach for the integration of chromatographic peaks (5). Another problem with SEC is related to a nonspecific binding of protein aggregates to the column matrix, as recently discussed (6).

The above-mentioned issues potentially affect the accuracy of SEC measurements. Thus, it has been suggested that the results of

* Corresponding author. Tel.: +81 6 6879 7440; fax: +81 6 6879 7442.
E-mail address: kfukui@bio.eng.osaka-u.ac.jp (K. Fukui).

1389-1723/$ – see front matter
http://dx.doi.org/10.1016/j.jbiosc.2012.07.021

the SEC method should be verified using different analytical techniques (7). Among alternatives to SEC method, analytical ultracentrifugation sedimentation velocity (AUC-SV) was found to be very suitable for this purpose (8).

The improvements in AUC instrumentation and data analysis packages have promoted an increase in the number of potential applications of AUC-SV (9–12). Particularly, it has been indicated as a valuable tool for monitoring antibody aggregation (8,13–16). Nevertheless, owing to the lower degree of reproducibility of AUC-SV results compared with SEC results, the implementation of AUC-SV to a routine characterization of pharmaceutical antibodies has not been successful until now. In the recent study presenting the summary opinion of the members of the protein characterization subcommittee of the European Immunogenicity Platform, it has been suggested that throughout the pharmaceutical development process, AUC should not be used for validation of SEC results but rather should be used as a complementary method for SEC (17).

The purpose of this study was to demonstrate that AUC-SV can very effectively be used for the characterization of marketed immunoglobulin preparations and to confirm the performance of SEC. Over the years, a number of studies have been performed using AUC-SV and SEC, as applied to custom monoclonal antibody formulations (13,14). In contrast, the present research was conducted using a wide range of available marketed products, consisting of four liquid formulations and three lyophilized formulations of pharmaceutical human immunoglobulin preparations. Based on the previous studies (18–20) and our own results (21), experimental and data analysis procedures for precise aggregation content measurement in immunoglobulin formulations using AUC-SV were developed. Following the established protocol, we confirmed that AUC-SV can very effectively be used to characterize marketed pharmaceutical products. To address the uncertainty that can result from application of different methods for chromatographic peak identification, we applied the vertical drop method and the Gaussian skim approach, implemented in the Empower II software to analyze SEC data. Although integration of chromatographic peaks using the vertical drop method consistently indicated a slightly greater amount of aggregates compared with the value estimated by using the Gaussian skim algorithm, we achieved good overall agreement between AUC-SV and SEC results.

MATERIALS AND METHODS

Human immunoglobulin preparations In the present study, four liquid and three lyophilized preparations of human immunoglobulins were used. Polyglobin-N 5% for intravenous injection (0.5 g/10 ml), a pH 4-treated acidic human normal immunoglobulin, was purchased from the Japanese Red Cross Society (Tokyo, Japan). Venoglobulin IH 5% for intravenous injection (0.5 g/10 ml), a polyethylene glycol-treated human normal immunoglobulin; Hebsbulin IH for intravenous injection (1000 units), a polyethylene glycol-treated human anti-HBs immunoglobulin; and Tetanobulin IH for intravenous injection (250 units), a polyethylene glycol-treated human tetanus immunoglobulin, were purchased from Benesis Corporation (Osaka, Japan). Glovenin-I for intravenous injection (500 mg), a freeze-dried polyethylene glycol-treated human normal immunoglobulin G, was purchased from Nihon Pharmaceutical Co., Ltd. (Tokyo, Japan). Gammagard for intravenous injection (2.5 g), a freeze-dried ion-exchange resin-treated human normal immunoglobulin, was purchased from Baxter Limited (Tokyo, Japan). Sanglopor for intravenous infusion (2.5 g), a freeze-dried pH 4-treated human immunoglobulin, was purchased from CSL Behring (Tokyo, Japan). For all lyophilized products, the immunoglobulin concentration in the reconstituted formulation was 50 mg/ml.

Size-exclusion chromatography SEC analysis was performed in triplicate using a high-performance liquid chromatography (HPLC) workstation (Alliance 1100 HPLC system) with a TSK gel G3000SW$_{XL}$ column (Tosoh Bioscience, Tokyo, Japan) under standard conditions. The separation was conducted at a flow rate of 0.5 ml/min at room temperature and was monitored by UV detection at 280 nm. The elution buffer consisted of 1 mM potassium phosphate, 3 mM sodium phosphate, and 155 mM sodium chloride at pH 7.4. A minimum reproducible volume of 5 µl of antibodies at formulation concentrations was injected into the HPLC system for analysis. This prevented excessive antibody dilution, as SEC itself is known to produce a high dilution of the sample that will tend to dissociate the reversible aggregates (22). An antibody mass recovery of 94% and higher was confirmed for all studied samples and was in agreement with the values from previous studies (14,23). Chromatographic data were processed by the Empower II chromatography data software (Waters, Tokyo, Japan) using the ApexTrack integration algorithm combined with either the vertical drop method or the Gaussian skim method. The integration parameters were set at default, and Detect Shoulders event was enabled. To estimate the fractional amount of each peak, the calculated peak area was divided by the total area that was obtained by summation of the areas of the peaks, including the solvent peak, where it was present.

Analytical ultracentrifugation sedimentation velocity AUC-SV analysis was performed according to the experimental routine especially designed for the present study. It addresses specific requirements to conduct the measurement of aggregation content in immunoglobulin preparations in a very precise manner. Thus, the sedimentation experiments were conducted in a ProteomeLab XL-I analytical ultracentrifuge (Beckman Coulter) equipped with a 4-hole An60 Ti rotor. Beckman Coulter 12-mm double-sector charcoal-filled epon centerpieces manufactured after July 2008, when an improved manufacturing process was implemented by Beckman Coulter (19), and quartz windows were used for the experiments. The cells filled with 430 µl of the prepared samples were placed in the rotor and thoroughly equilibrated at 20°C and 0 rpm for approximately 1 h before beginning data acquisition. Data were recorded at 40,000 rpm and 20°C using absorbance optics at 280 nm. The scanning was performed as quickly as possible between radial positions 5.9 and 7.2 cm, with a step size of 30 µm until the sample was completely sedimented.

AUC-SV analysis of the selected preparations was complicated by the non-ideality of the formulations, containing high concentrations of excipients such as sugars and sugar alcohols. Therefore, the antibody formulations were diluted to the concentration of approximately 0.5 mg/ml using buffer consisting of 1 mM potassium phosphate, 3 mM sodium phosphate, and 155 mM sodium chloride at pH 7.4. The antibody samples were prepared immediately before the AUC-SV measurement. In this way, any potential decrease in the amount of aggregates due to reversible dissociation was minimized. AUC-SV runs were performed in triplicate, with three data sets collected in each run. The same combination of rotor hole position, cell housing, windows, and centerpiece was used for all consecutive runs, as recommended previously (19). This practice helped us to identify the micro-deformation of the centerpiece systematically affecting the quality of the data acquired for the cell placed in rotor hole 3. Therefore, these data were excluded from further analysis.

The SEC analysis of the reconstituted lyophilized preparations of immunoglobulins indicated relatively slow time-dependent change in the distribution of monomeric/dimeric forms of antibody, which was negligible compared with the time of the first sedimentation experiment, performed immediately after reconstitution. However, as the time interval between the reconstitution and the beginning of the second and third experiments was longer, the distribution was significantly affected. Thus, the results of the AUC-SV analysis are presented as the mean values of six measurements performed in three independent runs for the liquid formulations and as the mean values of two measurements performed in one run for the freeze-dried formulations.

The data were analyzed using the C(*s*) method of SEDFIT ((24); http://www.analyticalultracentrifugation.com). For the analysis, the meniscus was set to the midpoint position of the absorbance spike corresponding to the air-sample boundary and was floated during the fit. It was confirmed that the fitted meniscus position was physically relevant and was still located in the vicinity of the maximum of absorbance spike. The sedimentation coefficient (*s*) range was chosen so that no partial peaks were presented at the edges of the s-range and was 1–15 S, 1–20 S, 1–25 S, or 1–30 S, respectively. A grid resolution was selected in a way that resolution of *s* values corresponded to 0.05 S. The frictional ratio was initialized at 1.4 and floated during the fitting procedure. A regularization level of 0.68 was used. The buffer density and viscosity were calculated using the SEDNTERP software and were 1.00516 g/ml and 1.0175 cP, respectively. The partial specific volume was kept at the SEDFIT default value of 0.73 cm^3/g, which in general provides a good estimate of the partial specific volume of proteins. The actual values could not be estimated owing to the polyclonal nature of the studied antibody formulations. The goodness of the obtained fits was evaluated by comparing the rmsd values of the resulting fits with the values obtained for the empty cells before the experiments. In this way, it was verified that all the fits had only a randomly distributed noise and that no systematic errors were introduced during the fitting routine. In addition, it was confirmed that no visible diagonal lines were present on the residuals bitmap. To estimate the relative abundance of the different species present in the samples, integration of the C(*s*) distributions was performed. The percentages of antibody monomers, oligomers, fragments, and albumin were calculated by dividing the corresponding peak area by the sum of the areas under all peaks.

RESULTS

Experimental routine for AUC-SV analysis of immunoglobulin preparations The development of an experimental routine for AUC-SV analysis of immunoglobulin preparations

followed two main phases: a systematic review of the available literature on the subject and testing of a theoretically designed protocol. First, based on the previous studies (18–20), a set of experimental parameters regarding rotor and cell components, sample concentration used for the analysis, optics applied for the detection, and software package for the data analysis were chosen. At the next step, the optimum rotational speed from the recommended range of 40,000–60,000 rpm was selected for AUC-SV analysis. Our previous study has shown that the hydrodynamic parameters of antibodies are affected by high rotational speed during sedimentation experiments, whereas the amount of dimeric antibody aggregate remained unaffected by the rotational speed (21). Thus, we excluded rotational speeds faster than 50,000 rpm from consideration, assuming that these high speeds can contribute to the imprecision of aggregation analysis. High-quality centerpieces, which have previously been shown to improve the precision of aggregates measurements, were Beckman Coulter charcoal-filled epon centerpieces. The Beckman Coulter Buyer's Guide recommends using the epon charcoal-filled centerpieces at speeds slower than 42,000 rpm. Finally, the possible presence of fast-sedimenting high-molecular weight aggregates was considered; thus a rotational speed of 40,000 rpm was selected for the AUC-SV experimental setup.

Aggregation analysis of liquid human immunoglobulin preparations The SEC chromatogram of Polyglobin (Fig. 1A) showed a major peak corresponding to the monomeric form of the antibody. The asymmetry of the monomer peak was attributed to the nonspecific binding of the highly concentrated antibody to the SEC column packing material (6), which is a common problem in protein chromatography. A shoulder peak eluted before the major peak suggested the presence of a dimeric component in the solution. When either integration algorithm was applied for the data analysis, the area under the dimeric peak was estimated to be approximately 0.8% of the total signal (Table 1). This estimate was lower compared with that obtained by AUC-SV analysis. In C(s) distribution (Fig. 1B), in addition to monomeric and dimeric peaks, minor peaks corresponding to antibody fragments and trimeric aggregates were observed. Nevertheless, the results of triplicate measurements showed that these species were present at amounts below the commonly accepted limit of AUC-SV quantification of 1% (25) and therefore could not be considered to be reliably measured. In addition, the standard deviation of the obtained values indicated low reliability of these estimates.

The fraction of dimeric aggregates present in the Venoglobulin formulation was higher than that estimated for Polyglobin (Table 1). Similar to Polyglobin, the AUC-SV analysis of Venoglobulin indicated the presence of trace amounts of fragments and trimeric aggregates below the accepted limit of quantification. The estimates of the total quantity of aggregates derived from AUC-SV measurements and integration of chromatogram using the Gaussian skim approach were in good agreement. The results of peak separation using the vertical drop method and the Gaussian skim approach were consistent, although the amount of dimeric aggregates calculated by the vertical drop method was slightly higher than that obtained by the Gaussian skim approach.

The results of AUC-SV and SEC obtained for Hebsbulin were in good agreement, indicating the presence of only monomeric and dimeric forms of the antibody (Fig. 1E and F). The amount of dimeric aggregates was estimated to be the highest by SEC with the vertical drop method (2.62%), followed by SEC with the Gaussian skim approach (2.54%), and AUC-SV (2.25%; Table 1).

The C(s) distribution of Tetanobulin showed two peaks corresponding to the monomeric and dimeric forms of the antibody (Fig. 1H). The amount of dimeric aggregates derived from the AUC-SV analysis was lower than the value obtained using the vertical drop method for chromatographic data analysis (Table 1). The SEC analysis detected a minor peak in the chromatogram corresponding to trimer/higher aggregates, which was not detected by AUC-SV (Fig. 1K). Integration of the chromatographic peaks showed that these species were present at amounts below the estimated limit of AUC-SV detection of 0.2% (25). Moreover, the obtained value was close to the limit of detection previously determined for SEC (TSK gel SEC Brochure – Tosoh Bioscience GmbH).

Aggregation analysis of lyophilized immunoglobulin preparations The two major peaks corresponding to the monomeric and dimeric forms of the antibody were detected by SEC and AUC-SV analyses of the Glovenin formulation. In the chromatogram (Fig. 1I), these peaks co-eluted and were baseline-unresolved. From integration of the chromatogram by using the vertical drop method, the amount of dimeric aggregates was estimated to be 1.18% higher compared with the estimate produced by the Gaussian skim integration algorithm and 1.39% higher compared with the estimate determined by the C(s) analysis of the AUC-SV data.

The chromatographic profile obtained for Gammagard indicated the presence of four major peaks corresponding to solvent, monomeric, dimeric, and trimeric forms of the antibody. The AUC-SV analysis also detected albumin and trace amounts of high-molecular weight aggregates. The amount of dimeric aggregates estimated by the vertical drop method of SEC chromatogram was significantly higher compared with that calculated using the Gaussian skim algorithm. However, the Gaussian skim algorithm failed to accurately resolve a minor peak corresponding to solvent preventing accurate quantification of the monomeric form of the antibody (Table 1).

There was a significant difference between the AUC-SV and SEC results obtained for Sanglopor independent of the integration approach applied to the SEC data analysis. Similar to other immunoglobulin preparations, the dimeric aggregates amount determined by the Gaussian skim algorithm was lower than that obtained by the vertical drop method. It is interesting that the amount of dimeric aggregates estimated by AUC-SV was lower than that calculated using the vertical drop method but was higher than that resulting from integration using the Gaussian skim approach. The AUC-SV analysis revealed the presence of two antibody fragments and trace amounts of high-molecular weight aggregates, which were not detected in the elution profile.

DISCUSSION

In the present study, the aggregate compositions of different preparations of human immunoglobulins were analyzed using AUC-SV and SEC with the vertical drop method and the Gaussian skim approach. Although AUC-SV and SEC degrees of precision differed, these two analytical techniques provided similar results in the quantification of aggregates confirming the complementary relationship between AUC-SV and SEC. As has been discussed (6,14,16,17), both SEC and AUC-SV methods can be used to quantify the aggregates in the pharmaceutical formulations. Due to its simplicity, speed, and reproducibility of obtained results, SEC is routinely used as a quality control method to evaluate the aggregation of pharmaceuticals. In contrast to SEC, AUC-SV does not conform to the requirements specified for the quality control methods because of the relatively low precision and repeatability. However, AUC-SV offers a significant advantage over SEC as it provides matrix-free separation of the solutes, and therefore, it can be performed to ensure that the sample's composition has not changed owing to interaction with the column packing material. In addition, larger soluble aggregates eluted in the void volume of the SEC column can be detected and characterized by AUC-SV (14).

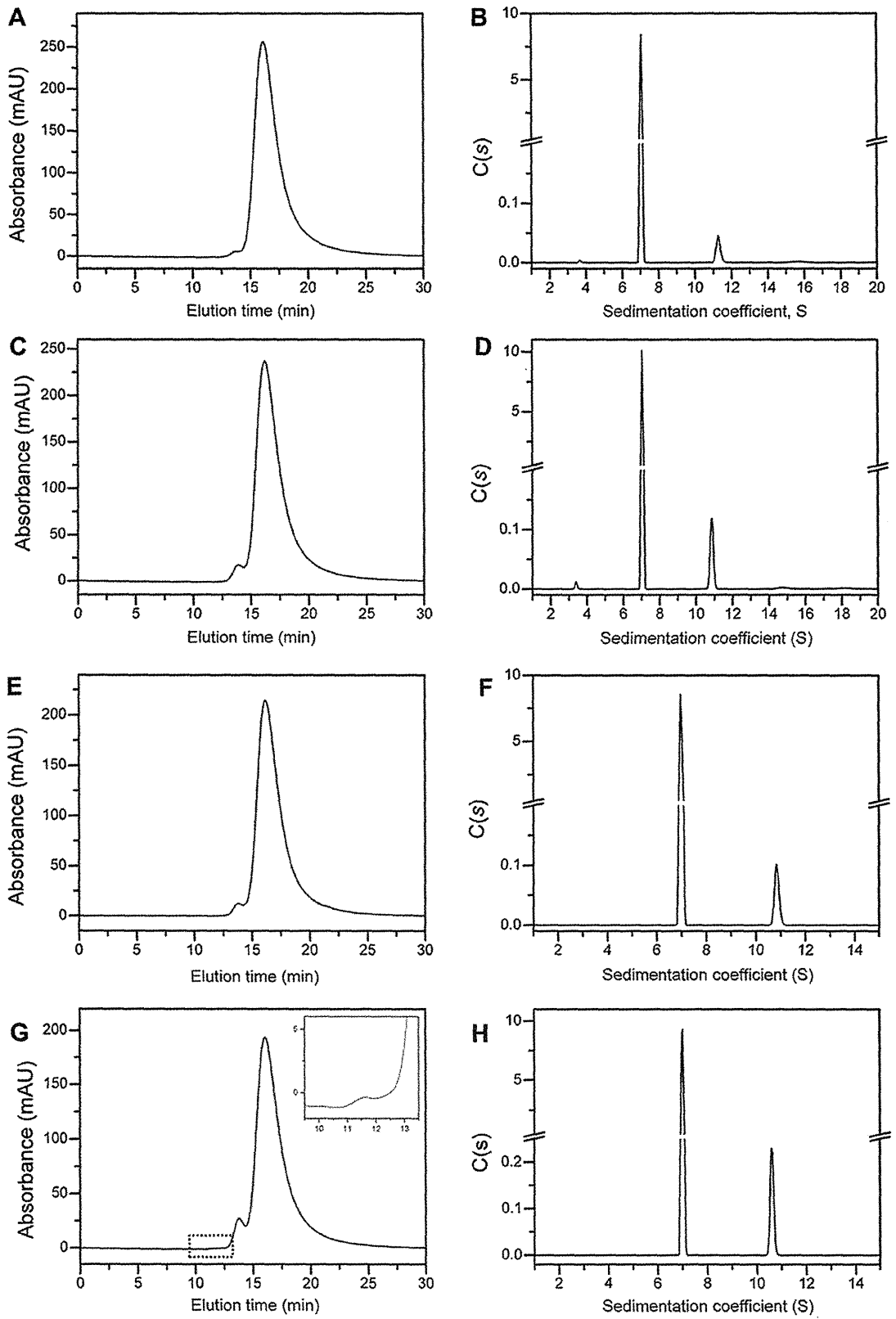

FIG. 1. Size-exclusion chromatograms and sedimentation coefficients distributions C(*s*) obtained for the following human immunoglobulin preparations: (A, B) Polyglobin, (C, D) Venoglobulin, (E, F) Hebsbulin, (G, H) Tetanobulin, (I, J) Glovenin, (K, L) Gammagard, and (M, N) Sanglopor. The insets in panels G and K show enlarged view of the boxed areas. The insets in panels L and N show the C(*s*) distributions with expanded vertical scale. The size-exclusion chromatograms and the continuous sedimentation coefficient distributions C(*s*) consistently showed the same number of peaks, with the exception of Sanglopor, for which the *C(s)* distribution indicated the presence of two peaks corresponding to antibody fragments, whereas these peaks were not seen in the SEC chromatogram.

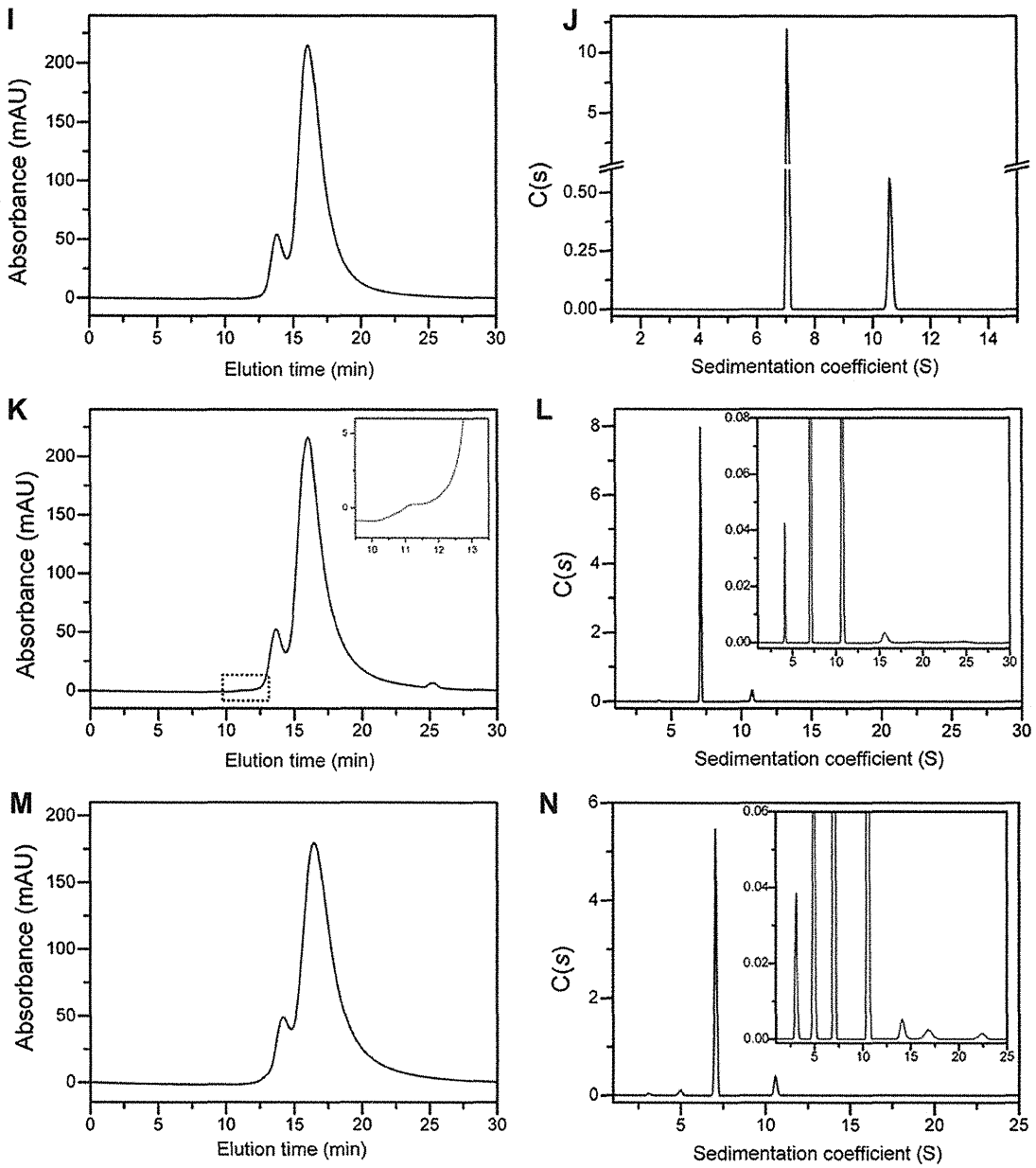

FIG. 1. (*continued*).

The results of the chromatographic analyses obtained using different integration approaches showed minimal variability for the solutions of Venoglobulin, Polyglobin, and Hebsbulin. For the other formulations used in this study, integration of the peaks using the vertical drop method systematically provided higher values of dimeric aggregate compared with those from the Gaussian skim approach. It was noted that with increase in the height of the valley between the unresolved peaks corresponding to monomer and dimer, the differences between estimates produced by the vertical drop method and the Gaussian integration approach increased. These differences were attributed to the differences in integration algorithms, and it was suggested that the Gaussian skim approach was inherently more accurate for overlapping peak separation than the traditional, vertical drop method. This conclusion is also supported by the AUC-SV results that showed better agreement with the results obtained using the Gaussian skim method, but not with the vertical drop method. However, in the case of Gammagard, the Gaussian skim method failed to accurately estimate the area under the small peak corresponding to solvent (Table 1) preventing correct quantification of the monomeric form of the antibody. A reasonably accurate result was obtained when tangential skim (algorithm that performs valley-to-valley extrapolation) (5) was applied, which is known to perform well when it is used to skim a much smaller and narrower peak from the large parent peak. However, similar to the result of the vertical drop method, the amount of dimeric aggregates was overestimated when the tangential skim approach was used. The analysis of the Gammagard chromatogram was complicated by the fact that the peaks could not conform to a single mathematical model, and the asymmetry and further overlapping of the peaks increased the complexity of the chromatogram.

The best way to eliminate measurement error is to increase the resolution of the chromatogram to obtain baseline separated peaks.

TABLE 1. Detailed quantitative summary of the results obtained by C(*s*) SEDFIT analysis of the AUC-SV data and by the vertical drop method and Gaussian skim algorithm analysis of the SEC data.

Product	Method	Albumin, %	Fragment, %	Monomer, %	Dimer, %	Trimer, %	HMW, %
Polyglobin	AUC[a]	–	0.33 ± 0.17	98.26 ± 0.27	1.27 ± 0.16	0.19 ± 0.07	–
	SEC-vertical drop[b]	–	–	99.20 ± 0.01	0.80 ± 0.01	–	–
	SEC-Gaussian skim[b]	–	–	99.20 ± 0.03	0.80 ± 0.03	–	–
Venoglobulin	AUC[a]	–	0.14 ± 0.02	97.24 ± 0.21	2.60 ± 0.21	0.18 ± 0.07	–
	SEC-vertical drop[b]	–	–	97.32 ± 0.08	2.68 ± 0.08	–	–
	SEC-Gaussian skim[b]	–	–	97.46 ± 0.07	2.54 ± 0.07	–	–
Hebsbulin	AUC[a]	–	–	97.75 ± 0.20	2.25 ± 0.20	–	–
	SEC-vertical drop[b]	–	–	97.45 ± 0.04	2.56 ± 0.04	–	–
	SEC-Gaussian skim[b]	–	–	97.47 ± 0.02	2.54 ± 0.02	–	–
Tetanobulin	AUC[a]	–	–	95.74 ± 0.21	4.26 ± 0.21	–	–
	SEC-vertical drop[b]	–	–	94.75 ± 0.11	5.15 ± 0.10	0.10 ± 0.01	–
	SEC-Gaussian skim[b]	–	–	95.51 ± 0.06	4.35 ± 0.06	0.14 ± 0.00	–
Glovenin	AUC[c]	–	–	90.76 ± 0.20	9.24 ± 0.20	–	–
	SEC-vertical drop[b]	–	–	89.37 ± 0.16	10.63 ± 0.16	–	–
	SEC-Gaussian skim[b]	–	–	90.55 ± 0.02	9.45 ± 0.02	–	–
Gammagard	AUC[c]	0.53 ± 0.13	–	92.05 ± 0.28	6.86 ± 0.26	0.34 ± 0.11	0.22 ± 0.04
	SEC-vertical drop[b]	1.57 ± 0.00[d]	–	88.61 ± 0.20	9.75 ± 0.14	0.11 ± 0.01	–
	SEC-Gaussian skim[b]	6.25 ± 0.25[d]	–	85.02 ± 0.06	8.40 ± 0.30	0.32 ± 0.04	–
Sanglopor	AUC[c]	–	1.07 ± 0.08 3.02 ± 0.26	85.40 ± 0.09	9.64 ± 0.09	0.47 ± 0.17	0.41 ± 0.02
	SEC-vertical drop[b]	–	–	89.69 ± 0.28	10.32 ± 0.28	–	–
	SEC-Gaussian skim[b]	–	–	91.34 ± 0.04	8.66 ± 0.04	–	–

[a] The data are the mean values of six measurements performed in three independent runs ± SD.
[b] The data are the mean values of triplicate measurements ± SD.
[c] The data are the mean values of two measurements performed in one run ± SD.
[d] The albumin peak was not detected. The reported value is the result of the solvent peak integration.

In general, this can be achieved by modifications of the mobile phase. However, the choice of optimum mobile phase is a tradeoff between resolution and accuracy. As has been discussed (6,22), adjustments of the mobile phase can increase the resolution and at the same time may affect the original aggregate distribution in the antibody formulation. In addition, by increasing the resolution between monomer and dimer, the resolution of higher oligomers can significantly be altered.

AUC-SV was extensively used for the characterization of antibody samples (16) and, in particular, was successfully applied to the aggregation analysis of pharmaceutical antibodies (20). In the present study, a very high degree of agreement was observed between AUC-SV and SEC results for liquid formulations of immunoglobulin. In contrast, the agreement was relatively poor in the case of reconstituted preparations. In these formulations, SEC measurements performed on consecutive days suggested the loss of monomer due to formation of dimeric aggregates. This process was shown to be relatively slow compared with the time course of the sedimentation experiment. Surprisingly, the amount of dimeric aggregates estimated using AUC-SV was lower than the value obtained by SEC. We concluded that in the reconstituted formulations used for the AUC-SV measurements, the equilibrium of the monomer–dimer reaction was shifted toward monomer formation owing to a hundred-fold dilution required to analyze these solutions.

In the case of Sanglopor, the AUC-SV analysis detected the presence of two fragments, which were not visible in the chromatogram (Fig. 1M). It is suggested that the highly asymmetrical large monomer peak eluted before the smaller fragments' peaks caused this effect. Another hypothesis was that the relatively long centrifugation times could cause the degradation of monomer into antibody fragments.

In conclusion, the results of AUC-SV and SEC were consistent and the degree of agreement was higher when the chromatographic data were analyzed by using the Gaussian skim approach (Fig. 2). Thus, the results of this study confirmed that AUC-SV is an appropriate complementary to SEC method for aggregate composition analysis and underscored the important role that the different integration methods can play in the quantitative interpretation of chromatographic results.

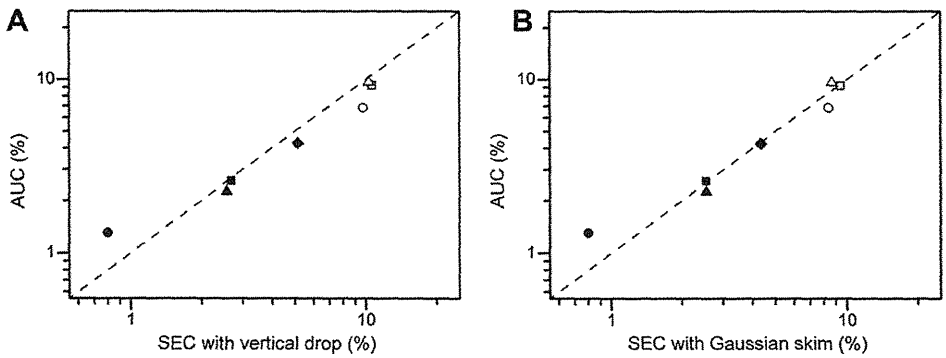

FIG. 2. Comparison of the dimeric aggregate amounts detected using AUC-SV and SEC with either (A) the vertical drop method or (B) the Gaussian skim approach. In each panel, the results for Polyglobin (filled circle), Venoglobulin (filled square), Hebsbulin (filled triangle), Tetanobulin (filled diamond), Gammagard (open circle), Sanglopor (open triangle), and Glovenin (open square) are shown. The degree of agreement between the AUC-SV and SEC results was higher when the Gaussian skim approach was applied for the chromatographic data analysis.

References

1. **Rosenberg, A. S.:** Effects of protein aggregates: an immunologic perspective, AAPS J., **8**, E501–E507 (2006).
2. **Meyer, V. R.:** Errors in the area determination of incompletely resolved chromatographic peaks, J. Chromatogr. Sci., **33**, 26–33 (1995).
3. **Foley, J. P.:** Systematic errors in the measurement of peak area and peak height for overlapping peaks, J. Chromatogr., **384**, 301–313 (1987).
4. **Meyer, V. R.:** Practical high-performance liquid chromatography, 5th ed., pp. 300–302. John Wiley & Sons, Ltd, UK (2010).
5. **Dyson, N.:** Chromatographic integration methods, 2nd ed., pp. 60–77. Royal Society of Chemistry, UK (1998).
6. **Arakawa, T., Ejima, D., Li, T., and Philo, J. S.:** The critical role of mobile phase composition in size exclusion chromatography of protein pharmaceuticals, J. Pharm. Sci., **99**, 1674–1692 (2010).
7. **Carpenter, J. F., Randolph, T. W., Jiskoot, W., Crommelin, D. J. A., Middaugh, C. R., and Winter, G.:** Potential inaccurate quantitation and sizing of protein aggregates by size exclusion chromatography: essential need to use orthogonal methods to assure the quality of therapeutic protein products, J. Pharm. Sci., **99**, 2200–2208 (2010).
8. **Berkowitz, S. A.:** Role of analytical ultracentrifugation in assessing the aggregation of protein biopharmaceuticals, AAPS J., **8**, E590–E605 (2006).
9. **Schuck, P.:** Diffusion-deconvoluted sedimentation coefficient distributions for the analysis of interacting and non-interacting protein mixtures, pp. 26–50, in: Scott, D. J., Harding, S. E., and Rowe, A. J. (Eds.), Analytical ultracentrifugation: techniques and methods. RSC Publishing, UK (2005).
10. **Harding, S. E.:** Analysis of polysaccharide size, shape and interactions, pp. 231–252, in: Scott, D. J., Harding, S. E., and Rowe, A. J. (Eds.), Analytical ultracentrifugation: techniques and methods. RSC Publishing, UK (2005).
11. **Demeler, B., Brookes, E., Wang, R., Schirf, V., and Kim, C. A.:** Characterization of reversible associations by sedimentation velocity with UltraScan, Macromol. Biosci., **10**, 775–782 (2010).
12. **Cole, J. L., Correia, J. J., and Stafford, W. F.:** The use of analytical sedimentation velocity to extract thermodynamic linkage, Biophys. Chem., **159**, 120–128 (2011).
13. **Arakawa, T., Philo, J. S., Ejima, D., Tsumoto, K., and Arisaka, F.:** Aggregation analysis of therapeutic proteins, Part 2: analytical ultracentrifugation and dynamic light scattering, Bioprocess Int., **5**, 36–47 (2007).
14. **Gabrielson, J. P., Brader, M. L., Pekar, A. H., Mathis, K. B., Winter, G., Carpenter, J. F., and Randolph, T. W.:** Quantitation of aggregate levels in a recombinant humanized monoclonal antibody formulation by size-exclusion chromatography, asymmetrical flow field flow fractionation, and sedimentation velocity, J. Pharm. Sci., **96**, 268–279 (2007).
15. **Liu, J., Andya, J. D., and Shire, S. J.:** A critical review of analytical ultracentrifugation and field flow fractionation methods for measuring protein aggregation, AAPS J., **22**, E580–E589 (2006).
16. **Philo, J. S.:** A critical review of methods for size characterization of non-particulate protein aggregates, Curr. Pharm. Biotechnol., **10**, 359–372 (2009).
17. **den Engelsman, J., Garidel, P., Smulders, R., Koll, H., Smith, B., Bassarab, S., Seidl, A., Hainzl, O., and Jiskoot, W.:** Strategies for the assessment of protein aggregates in pharmaceutical biotech product development, Pharm. Res., **28**, 920–933 (2011).
18. **Pekar, A. and Sukumar, M.:** Quantitation of aggregates in therapeutic proteins using sedimentation velocity analytical ultracentrifugation: practical considerations that affect precision and accuracy, Anal. Biochem., **367**, 225–237 (2007).
19. **Gabrielson, J. P., Arthur, K. K., Stoner, M. R., Winn, B. C., Kendrick, B. S., Razinkov, V., Svitel, J., Jiang, Y., Voelker, P. J., Fernandes, C. A., and Ridgeway, R.:** Precision of protein aggregation measurements by sedimentation velocity analytical ultracentrifugation in biopharmaceutical applications, Anal. Biochem., **396**, 231–241 (2010).
20. **Gabrielson, J. P. and Arthur, K. K.:** Measuring low levels of protein aggregation by sedimentation velocity, Methods, **54**, 83–91 (2011).
21. **Krayukhina, E., Uchiyama, S., and Fukui, K.:** Effects of rotational speed on the hydrodynamic properties of pharmaceutical antibodies measured by analytical ultracentrifugation sedimentation velocity, Eur. J. Pharm. Sci., **47**, 367–374 (2012).
22. **Philo, J. S.:** Is any measurement method optimal for all aggregate sizes and types? AAPS J., **8**, E564–E571 (2006).
23. **Eberlein, G. A.:** Quantitation of proteins using HPLC-detector response rather than standard curve comparison, J. Pharm. Biomed. Anal., **13**, 1263–1271 (1995).
24. **Schuck, P.:** Size-distribution analysis of macromolecules by sedimentation velocity ultracentrifugation and Lamm equation modeling, Biophys. J., **78**, 1606–1619 (2000).
25. **Brown, P. H., Balbo, A., and Schuck, P.:** A Bayesian approach for quantifying trace amounts of antibody aggregates by sedimentation velocity analytical ultracentrifugation, AAPS J., **10**, 481–493 (2008).

Jpn. J. Infect. Dis., 66, 561-563, 2013

Laboratory and Epidemiology Communications

Virological Analysis of a Regional Mumps Outbreak in the Northern Island of Japan—Mumps Virus Genotyping and Clinical Description

Kazuki Okajima[1]*, Kenichi Iseki[1], Shin Koyano[2], Atsushi Kato[3], and Hiroshi Azuma[2]

[1]Fukagawa City Hospital, Fukagawa 074-0006;
[2]Asahikawa Medical University, Asahikawa 078-8510; and
[3]National Institute of Infectious Diseases, Tokyo 208-0011, Japan

Communicated by Makoto Takeda

(Accepted August 20, 2013)

Mumps is an acute, contagious, vaccine-preventable disease caused by mumps virus (MuV) and is typically characterized by swelling of either or both parotid glands. A mumps epidemic occurs every 3–5 years in non-vaccinated populations, and humans are the only natural hosts for MuV, which is transmitted by the respiratory route and replicates primarily in the upper respiratory mucosal epithelium. Primary replication leads to viremia and triggers secondary viral replication (1). Parotitis is not, however, a necessary component of mumps symptoms. MuV can display neurovirulence. MuV can also enter the cerebrospinal fluid (CSF) through the choroid plexus, leading to a form of aseptic meningitis in up to approximately 10% of cases. More serious complications, such as deafness and encephalitis, occur less frequently and up to 30% of infections are asymptomatic or display only non-specific respiratory symptoms. Furthermore, reinfection with mumps has been confirmed in serological studies (2,3) and a significant portion of adult sudden sensorineural deafness is reportedly related to MuV infection (4).

In Japan, 5 mumps vaccines (genotype B) are currently licensed, and single dose is distributed on a voluntary basis (5), with a coverage rate of approximately 23% (6). However, herd immunity level is insufficient to prevent epidemics; therefore, mumps outbreaks in children repeat every several years.

MuV is a member of the genus *Rubulavirus* of the family *Paramyxoviridae*. Eight proteins, the nucleocapsid (N), V, phospho (P), matrix (M), fusion (F), small hydrophobic (SH), hemagglutinin-neuraminidase (HN), and large (L) proteins, are coded by 7 genes. The SH gene sequence is highly variable and is, therefore, used for MuV genotyping (7–9).

Fukagawa city (coordinates: 43°43′N, 142°2′E) is a relatively isolated rural region in Hokkaido, Japan, with a population of approximately 23,000. From April to August 2010, a total of 212 patients were diagnosed with mumps in the pediatric department of our hospital. In January 2011, 3 additional patients were diagnosed; the age range of these 215 patients was 1–19 years, and they had no significant medical history of immunodeficiency, malignancy, or developmental delay. Diagnosis was made on the basis of typical clinical manifestations and/or laboratory test results of serological study or amylase in the serum or urine. Seventeen patients were hospitalized; of these, 10 were diagnosed with meningitis, 3 with orchitis, and 1 with hepatitis. Two unrelated patients developed audiometry-con-

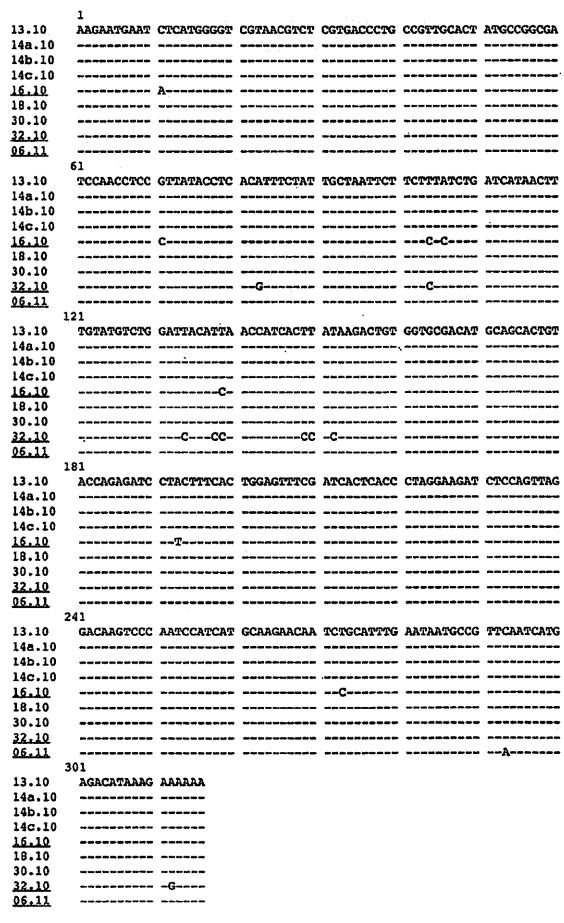

Fig. 1. Nucleotide sequences of SH gene detected in this study in chronological order. Left column shows week and year part of strain names. From top to bottom, AB725762.1, AB725761.1, AB725764.1, AB725766.1, AB725763.1, AB725760.1, AB725759.1, AB725765.1, and AB725767.1. Numbers above row denote nucleotide position. Underlined strains are not identical to index sequence.

*Corresponding author: Present address: Department of Pediatrics, Asahikawa Medical University, Midorigaoka E 2Jo, Asahikawa 078-8510, Japan. Tel: +81-166-68-2481, Fax: +81-166-68-2489, E-mail: okaji5p@asahikawa-med.ac.jp

firmed unilateral hearing loss as a sequela. One of these patients who developed hearing loss was positive for meningitis despite a vaccine history 9 years prior to the episode. According to this patient's medical record, Torii strain vaccine was administrated. On admission, anti-mumps IgG and IgM titers were measured using an EIA mumps kit (Denka Seiken, Tokyo, Japan), in which the MuV Enders strain was used as an antigen. The IgG titer (reference range: positive at a titer of 4 or more) was 13.7, and the IgM titer (reference range: positive at a titer of 1.2 or more) was below the detectable limit. The other patient was not vaccinated but did not show clinical signs of meningitis. Because 2 patients with hearing loss were observed, virological analysis of several stored samples (13 CSF's and 3 throat swabs) was performed to discern any underlying factors. All analyses were anonymously performed and complaint with the national guidelines for clinical research.

Nucleic acid detection and genotyping of MuV were performed as described previously (7). In brief, using a standard technique, the SH gene was RT-PCR amplified from CSF or throat swab samples after RNA isolation (Roche Diagnostics, Tokyo, Japan), using the primer pair "tcaagtagtgtcgatgatctc" and "aggtggcatt gtctgacattg" corresponding to the nucleotides 6130–6150 and 6656–6636, respectively, of NC_002200.1. A specific 526-bp band was amplified and sequenced. Multiple sequence alignment and phylogenetic analysis by the neighbor-joining method were performed using GENETYX-MAC (GENETYX Co., Tokyo, Japan). Nine of 13 CSF samples were successfully analyzed (GenBank accession numbers, AB725759.1–67.1), but none of the throat swab samples were suitable for analysis.

The six samples collected in April, May, and August 2010 had identical sequences, while the other 3 samples collected in April, and August 2010 and January 2011 revealed slightly different sequences (Fig. 1). The latter sequences were detected at either the beginning or end of the outbreak. All of these sequences were determined as genotype G by phylogenetic analysis (Fig. 2). None of the samples from the 3 vaccinated patients were successfully analyzed due to amplification failure. Nonetheless, our success rate was comparable with that of previous reports (9,10).

Mumps outbreaks, even among vaccinated populations, have recently been reported worldwide, including in the UK, the US, the Netherlands, and Canada (10–14). In the present outbreak, we detected MuV genotype G, which has been the predominant genotype commonly detected in recent outbreaks. The majority of MuV strains we detected were identical at the SH

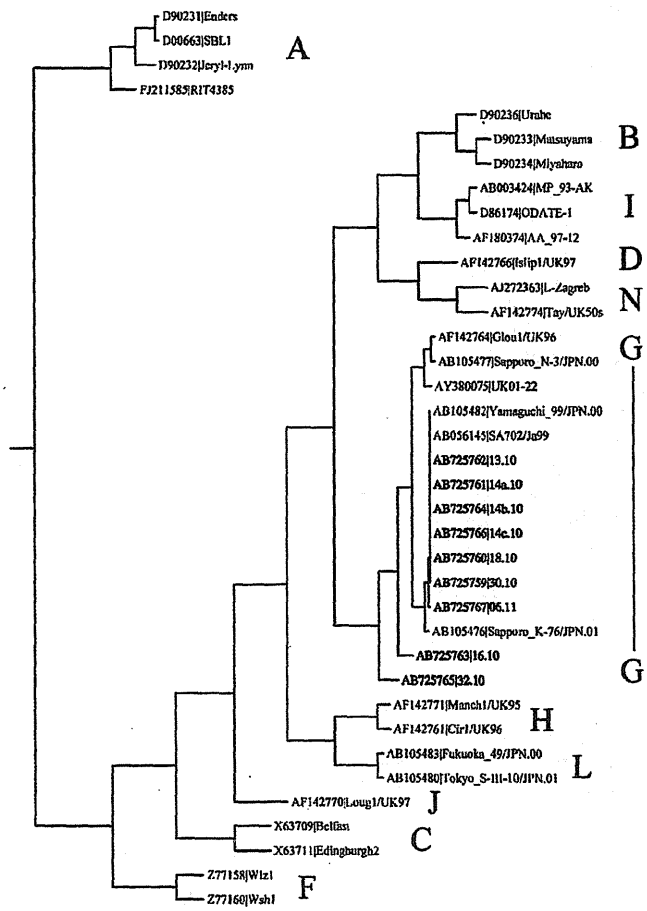

Fig. 2. Phylogenetic analysis of selected MuV strains. Strains detected in this study are in boldface. Capital letters denote MuV genotype.

gene level to those previously detected in geographically and chronologically distant areas of Yamaguchi (AB105482.1) and Saitama (AB056145.1), Japan (15,16). Although not identical, 2 other MuV genotype G strains (AB105476.1-77.1) were isolated in Sapporo, Japan, which is located approximately 100 km from Fukagawa on the same island. One finding of interest is that one strain isolated in the UK (AF142764.1) was phylogenetically similar to the strains we detected.

MuV genotypes H and D were detected in South Korea (17) and the Netherlands (18), respectively. In the present study, only genotype G was detected, with minor variations observed at the beginning and end of the outbreak. A short-time survey of vaccine coverage in the Fukagawa area revealed a rate of approximately 30%, which was slightly higher than the nationwide rate. Almost 30% of patients in this study were vaccinated (data not shown). Overall, the clinical courses of the vaccinated patients were mild, except for the patient who developed hearing loss. The anti-mumps serological study suggested secondary vaccine failure rather than primary vaccine failure.

The incidence of hearing loss in mumps patients is reportedly 0.001%-1.0% (19-21). The rate in the present study was 0.93% (2/215), which was comparable with the highest incidence thus far reported (11). Another study from Japan also reported a high rate of hearing problems. There are several other reported cases of hearing loss after mumps vaccination (20,22,23). We have been unable to conduct a survey to assess sensorineural deafness in this area.

Genotype mismatch between vaccine and epidemic virus strains has been often discussed in association with several outbreaks (24,25), demonstrating that antibodies against a vaccine strain failed to prevent infection by other strains. On the other hand, some publications have reported that antibodies raised against vaccine strains were able to neutralize other genotype strains (26,27). Antibodies raised against the Enders strain (genotype A) can be successfully employed in detection kits. We observed that a MuV genotype B vaccine failed to prevent the manifestations of mumps (genotype G) in a significant portion of a population, although the vaccine was able to ameliorate the clinical course of the disease. Our current mumps vaccine scheme may not be optimal. We were unable to discern any significant factors in either the host or viral side in this mumps outbreak with a high sequela rate. Further elucidation of the virological and epidemiological backgrounds of this occurrence was beyond the scope of this study.

Conflict of interest None to declare.

REFERENCES

1. Rubin, S.A. and Carbone, K.M. (2011): Mumps. p. 1608-1610. *In* D.L. Longo, A.S. Fauci, D.L. Kasper, et al. (ed.), Harrison's Principles of Internal Medicine. 18th ed. McGraw-Hill, N.Y.
2. Vinagre, C., Martínez, M.J., Avendano, L.F., et al. (2003): Virology of infantile chronic recurrent parotitis in Santiago de Chile. J. Med. Virol., 70, 459-462.
3. Yoshida, N., Fujino, M., Miyata, A., et al. (2008): Mumps virus reinfection is not a rare event confirmed by reverse transcription loop-mediated isothermal amplification. J. Med. Virol., 80, 517-523.
4. Chau, J.K., Lin, J.R., Atashband, S., et al. (2010): Systematic review of the evidence for the etiology of adult sudden sensorineural hearing loss. Laryngoscope, 120, 1011-1021.
5. Sawada, A., Yamaji, Y., Nakayama, T. (2013): Mumps Hoshino and Torii vaccine strains were distinguished from circulating wild strains. J. Infect. Chemother., 19, 480-485.
6. Baba, K., Okuno, Y., Tanaka-Taya, K., et al. (2011): Immunization coverage and natural infection rates of vaccine-preventable diseases among children by questionnaire survey in 2005 in Japan. Vaccine, 29, 3089-3092.
7. Takeuchi, K., Tanabayashi, K., Hishiyama, M., et al. (1991): Variations of nucleotide sequences and transcription of the SH gene among mumps virus strains. Virology, 181, 364-366.
8. Jin, L., Rima, B., Brown, D., et al. (2005): Proposal for genetic characterisation of wild-type mumps strains: preliminary standardisation of the nomenclature. Arch. Virol., 150, 1903-1909.
9. Kidokoro, M., Tuul, R., Komase, K., et al. (2011): Characterization of mumps viruses circulating in Mongolia: identification of a novel cluster of genotype H. J. Clin. Microbiol., 49, 1917-1925.
10. Carr, M.J., Moss, E., Waters, A., et al. (2010): Molecular epidemiological evaluation of the recent resurgence in mumps virus infections in Ireland. J. Clin. Microbiol., 48, 3288-3294.
11. Whelan, J., van Binnendijk, R., Greenland, K., et al. (2010): Ongoing mumps outbreak in a student population with high vaccination coverage, Netherlands, 2010. *Euro Surveill.*, 15, pii= 19554.
12. Centers for Disease Control and Prevention (CDC). (2010): Update: Mumps Outbreak—New York and New Jersey, June 2009-January 2010. MMWR Morb. Motal. Wkly. Rep., 59, 125-129.
13. Deeks, S.L., Lim, G.H., Simpson, M.A., et al. (2011): An assessment of mumps vaccine effectiveness by dose during an outbreak in Canada. Can. Med. Assoc. J., 183, 1014-1020.
14. Echevarria, J.E., Castellanos, A., Sanz, J.C., et al. (2010): Circulation of mumps virus genotypes in Spain from 1996 to 2007. J. Clin. Microbiol., 48, 1245-1254.
15. Uchida, K., Shinohara, M., Shimada, S., et al. (2001): Characterization of mumps virus isolated in Saitama prefecture, Japan, by sequence analysis of the SH gene. Microbiol. Immunol., 45, 851-855.
16. Inou, Y., Nakayama, T., Yoshida, N., et al. (2004): Molecular epidemiology of mumps virus in Japan and proposal of two new genotypes. J. Med. Virol., 73, 97-104.
17. Lee, J.Y., Na, B.K., Kim, J.H., et al. (2004): Regional outbreak of mumps due to genotype H in Korea in 1999. J. Med. Virol., 73, 85-90.
18. Kaaijk, P., van der Zeijst, B.A., Boog, M.C., et al. (2008): Increased mumps incidence in the Netherlands: review on the possible role of vaccine strain and genotype. *Euro Surveill.*, 13, pii= 18914.
19. Hviid, A., Rubin, S., Mühlemann, K. (2008): Mumps. Lancet, 371, 932-944.
20. Asatryan, A., Pool, V., Chen, R.T., et al. (2008): Live attenuated measles and mumps viral strain-containing vaccines and hearing loss: Vaccine Adverse Event Reporting System (VAERS), United States, 1990-2003. Vaccine, 26, 1166-1172.
21. Kawashima, Y., Ihara, K., Nakamura, M., et al. (2005): Epidemiological study of mumps deafness in Japan. Auris Nasus Larynx, 32, 125-128.
22. Nabe-Nielsen, J. and Walter, B. (1988): Unilateral deafness as a complication of the mumps, measles, and rubella vaccination. Brit. Med. J., 297, 489.
23. Kaga, K., Ichimura, K. and Ihara, M. (1998): Unilateral total loss of auditory and vestibular function as a complication of mumps vaccination. Int. J. Pediatr. Otorhinolaryngol., 43, 73-75.
24. Boga, J.A., de Oña, M., Fernández-Verdugo, A., et al. (2008): Molecular identification of two genotypes of mumps virus causing two regional outbreaks in Asturias, Spain. J. Clin. Virol., 42, 425-428.
25. Nöjd, J., Tecle, T., Samuelsson, A., et al. (2001): Mumps virus neutralizing antibodies do not protect against reinfection with a heterologous mumps virus genotype. Vaccine, 19, 1727-1731.
26. Rubin, S., Mauldin, J., Chumakov, K., et al. (2006): Serological and phylogenetic evidence of monotypic immune responses to different mumps virus strains. Vaccine, 24, 2662-2668.
27. Rubin, S.A., Qi, L., Audet, S.A., et al. (2008): Antibody induced by immunization with the Jeryl Lynn mumps vaccine strain effectively neutralizes a heterologous wild-type mumps virus associated with a large outbreak. J. Infect. Dis., 198, 508-515.

JVI
Journals.ASM.org

TMPRSS2 Is an Activating Protease for Respiratory Parainfluenza Viruses

Masako Abe,[a] Maino Tahara,[a] Kouji Sakai,[a] Hiromi Yamaguchi,[e] Kazuhiko Kanou,[b] Kazuya Shirato,[a] Miyuki Kawase,[a] Masahiro Noda,[a,b] Hirokazu Kimura,[b] Shutoku Matsuyama,[a] Hideo Fukuhara,[f] Katsumi Mizuta,[d] Katsumi Maenaka,[f] Yasushi Ami,[c] Mariko Esumi,[e] Atsushi Kato,[a] Makoto Takeda[a]

Department of Virology 3,[a] Infectious Disease Surveillance Center,[b] and Division of Experimental Animal Research,[c] National Institute of Infectious Diseases, Tokyo, Japan; Yamagata Prefectural Institute of Public Health, Yamagata, Japan[d]; Department of Pathology, Nihon University School of Medicine, Itabashi-ku, Tokyo, Japan[e]; Laboratory of Biomolecular Science, Faculty of Pharmaceutical Sciences, Hokkaido University, Hokkaido, Japan[f]

Here, we show that human parainfluenza viruses and Sendai virus (SeV), like other respiratory viruses, use TMPRSS2 for their activation. The membrane fusion proteins of respiratory viruses often possess serine and glutamine residues at the P2 and P3 positions, respectively, but these residues were not critical for cleavage by TMPRSS2. However, mutations of these residues affected SeV growth in specific epithelial cell lines, suggesting the importance of these residues for SeV replication in epithelia.

In general, enveloped viruses initiate their infection by attaching to receptors on host cells, with subsequent membrane fusion between the virus envelope and the host cell membrane. The fusion process is mediated by a specialized surface glycoprotein, which is often synthesized as an inactive precursor and undergoes endoproteolysis by a host cell protease for activation. Recent studies have suggested that some type II transmembrane serine proteases (TTSPs), including TMPRSS2, human airway trypsin-like protease (HAT), TMPRSS4, and matriptase, are responsible for cleavage of the hemagglutinin (HA) protein of influenza A virus (IAV) in the human airway (1–6). Among these, TMPRSS2 has also been shown to proteolytically activate the F protein of human metapneumovirus (HMPV) (7). Severe acute respiratory syndrome (SARS) coronavirus (CoV), NL63 CoVs, and the novel human CoV (HCoV) EMC also use TMPRSS2 for their spike protein activation (8–13). Here, we studied the activation of respiratory parainfluenza viruses (human parainfluenza viruses [HPIVs] and Sendai virus [SeV]) by TMPRSS2.

HPIV1, HPIV4a, and HPIV4b generally require trypsin (trypsin dependent) to undergo multiple rounds of infection in most established cell lines, whereas some strains of HPIV2 and HPIV3 spread efficiently in cell lines in the absence of trypsin (trypsin independent) because they use the ubiquitous furin protease (14). HPIV1 (2272-Yamagata-2009 strain), HPIV4a (M-25 strain), HPIV4b (CH19503 strain), and trypsin-dependent HPIV2 (2331-Yamagata-2009 strain) and HPIV3 (1835-Yamagata-2009 strain) were used in the present study. In the absence of trypsin, none of these HPIV strains produced plaques in Vero cells, whereas all HPIVs showed plaque formation clearly in Vero/TMPRSS2 cells, which constitutively express TMPRSS2 (Fig. 1A). In a previous study (7), we generated Vero/TMPRSS2 cells by cotransfecting Vero cells with a TMPRSS2 expression vector, pCA7-TMPRSS2, in which EcoRI and NotI sites were used for cloning, and the *neo* gene-bearing vector pCXN2. For multistep growth experiments, Vero/TMPRSS2 and Vero cells were infected with HPIVs at a multiplicity of infection (MOI) of 0.01. All HPIVs replicated efficiently in Vero/TMPRSS2 cells, even in the absence of trypsin (Fig. 1B). Analyses by SDS-PAGE followed by immunoblotting demonstrated cleavage of the F proteins of HPIVs in Vero/TMPRSS2 cells, but not in Vero cells, in the absence of trypsin (Fig. 1C). In these assays, rabbit antisera raised against peptides corresponding to the cytoplasmic regions of the HPIV1, HPIV3, and HPIV4 F proteins (VRRLLVMINSTNNSPINAYTLESRMRN PYM, IIIIAVKYYRIQKRNRVDQNDKPYVLTNK, and EVKNVA RNQRLNRDADLFYKIPSQIPVPR, respectively) and a peroxidase-conjugated secondary antibody were used. Polyvinylidene difluoride (PVDF) membranes, on which polypeptides from cell lysates were blotted, were treated with the ECL Plus reagent (Amersham Biosciences), and chemiluminescence signals on the membrane were detected and visualized with a VersaDoc 3000 imager (Bio-Rad, Hercules, CA) (Fig. 1C). For analysis of SeV, a recombinant wild-type SeV expressing red fluorescent protein [SeV-RFP(wt)] was used. To generate SeV-RFP(wt), the RFP gene was inserted into the 3′-end-proximal first locus of the SeV genome, which is encoded by an expression plasmid, generating the full-length SeV genome plasmid pSeV-RFP (15, 16). SeV-RFP(wt) was then generated by using a reverse-genetics technique (15). In the absence of trypsin, SeV-RFP(wt) failed to undergo multiple rounds of infection in Vero cells, whereas it propagated efficiently in Vero/TMPRSS2 cells (Fig. 1D and E). Analyses by SDS-PAGE and immunoblotting also demonstrated cleavage of the F protein of SeV-RFP(wt) in Vero/TMPRSS2 cells, but not in Vero cells, in the absence of trypsin (Fig. 1F). In this assay, a rabbit antiserum raised against the cytoplasmic region of the SeV F protein (RIPR DTYTLEPKIRHMYTNGGFDAMAEKR) was used. Consistently with these data, SeV particles released from Vero/TMPRSS2 cells possessed cleaved F proteins, even in the absence of trypsin (Fig. 1G). On the other hand, SeV particles released from Vero cells cultured in the absence of trypsin possessed uncleaved F proteins (Fig. 1G). These virus particles with uncleaved F proteins were

Received 3 June 2013 Accepted 14 August 2013
Published ahead of print 21 August 2013
Address correspondence to Atsushi Kato, akato@nih.go.jp, or Makoto Takeda, mtakeda@nih.go.jp.
M. Abe and M. Tahara contributed equally to this work.

doi:10.1128/JVI.01490-13

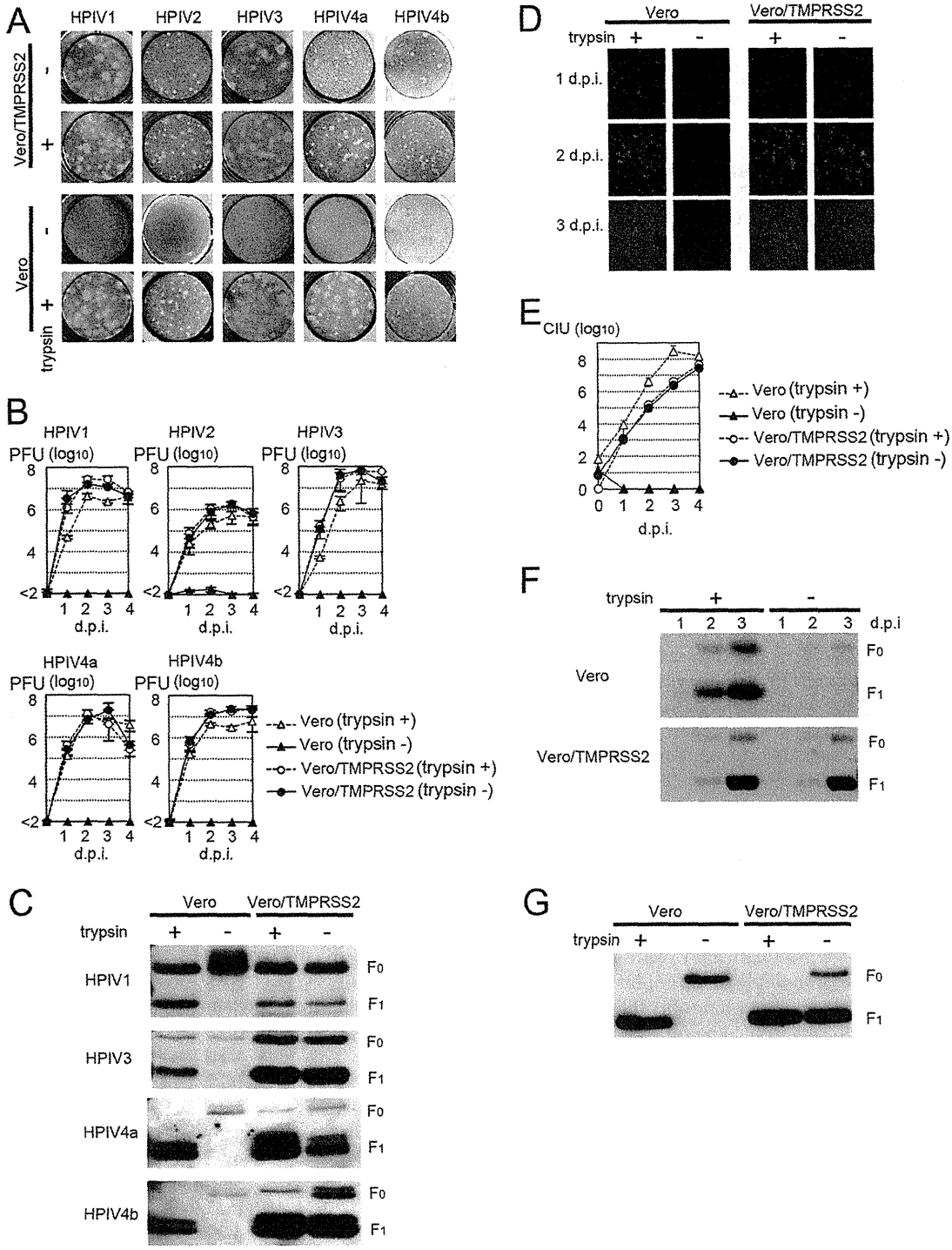

FIG 1 Proteolytic activation of HPIVs and SeV by TMPRSS2. (A) Plaque formation of HPIVs in Vero and Vero/TMPRSS2 cells in the presence or absence of trypsin. (B) Replication kinetics of HPIVs in Vero and Vero/TMPRSS2 cells. Cells were infected with HPIVs at an MOI of 0.01, cultured in the presence or absence of trypsin, and examined for their virus titers (PFU) daily. d.p.i., days postinfection. (C) Detection of HPIV F proteins by immunoblotting. Vero and Vero/TMPRSS2 cells infected with HPIVs in the presence or absence of trypsin were lysed in radioimmunoprecipitation assay (RIPA) buffer and subjected to SDS-PAGE and immunoblotting for detection of the F proteins (indicated as F_0 and F_1). (D) Detection of SeV-RFP(wt)-infected cells. Monolayers of Vero and Vero/TMPRSS2 cells were infected with SeV-RFP(wt) at an MOI of 0.01 and observed daily using a fluorescence microscope. (E) Replication kinetics of SeV-RFP(wt) in Vero and Vero/TMPRSS2 cells. Cells were infected with SeV-RFP(wt) at an MOI of 0.01, cultured in the presence or absence of trypsin, and examined for their virus titers (cell infectious units [CIU]) daily. (F) Detection of SeV F proteins in infected cells by immunoblotting. Vero and Vero/TMPRSS2 cells infected with SeV-RFP(wt) in the presence or absence of trypsin were lysed in RIPA buffer and subjected to SDS-PAGE and immunoblotting for detection of the F proteins. (G) Detection of SeV F proteins in virus particles by immunoblotting. Vero and Vero/TMPRSS2 cells were infected with SeV-RFP(wt) in the presence or absence of trypsin, and virus particles released from these cells were purified and subjected to SDS-PAGE and immunoblotting for detection of the F proteins.

TABLE 1 Residues of the cleavage site in virus membrane fusion proteins

Virus	Residue(s) at[a]: P7	P6	P5	P4	P3	P2	P1	P′1	P′2	P′3
HMPV	E	N	P	R	Q	S	R	F	V	L
SeV	A	D/G	A/V	P	Q	S	R	F	F	G
HPIV1	A/N	D	N/V	P	Q	S/T	R	F	F	G
HPIV2 (trypsin dependent)	T	A/K/T	P/T	R	Q	E	R	F	A	G
HPIV2 (trypsin independent)	T	K/T	T	R	Q	K	R	F	A	G
HPIV3 (trypsin dependent)	T	D	P	R	T	E	R	F	F	G
HPIV3 (trypsin independent)	T	D/N	P	R/T	T	K/R	R	F	F	G
HPIV4a	S	S	E	I	Q	S	R	F	F	G
HPIV4b	S	S	E	I	Q	S	R	F	F	G
IAV H1 subtype	I/V	P	S	I	Q	S	R	G	L	F
IAV H2 subtype	I/V	P	Q	I	E	S	R	G	L	F
IAV H3 subtype	I/V	P	E	K	Q	T	R	G	I/L	F
IAV H4 subtype	I	P	E	K	A	T	R	G	L	F
IAV H5 subtype	V	P	Q	R	E/K	T	R	G	L	F
IAV H6 subtype	I/V	P	Q	I	E	T	R	G	L	F
IAV H7 subtype	P	E	I	P	K	G	R	G	L	F
IAV H8 subtype	T	P	S	I/V	E	P	K/R	G	L	F
IAV H9 subtype	V	P	A	A/V	S	D	R	G	L	F
IAV H10 subtype	P	E	I	M	Q	G	R	G	L	F
IAV H11 subtype	V	P	A	I	A	S/T	R	G	L	F
IAV H12 subtype	V	P	Q	A/V	Q	D/N	R	G	L	F
IAV H13 subtype	V	P	A/T	I	A/S	N/S	R	G	L	F
IAV H14 subtype	I	P	G	K	Q	A	K	G	L	F
IAV H15 subtype	P	E	K	I	R	T	R	G	L	F
IAV H16 subtype	V	P	S	I/V	G/N/S/V	E	R	G	L	F
NDV (avirulent)	G	E/G	G	K/R	Q	G	R	L	I	G
Avian paramyxovirus type 2	F	D	K	P	A	S	R	F	V	G
Avian paramyxovirus type 3	Q	A/P	R	P	R/S	G	R	L	F	G
Avian paramyxovirus type 4	D/E	A/V	D	I	Q	P	R	F	I	G
Avian paramyxovirus type 6	H/N	P/S	A/I	P/R	E	P	R	L	I/V	G

[a] Serine and glutamine residues at P2 and P3 are underlined.

incapable of entering cells, even when the target cells expressed TMPRSS2 (data not shown). Thus, TMPRSS2 did not activate the F protein of the incoming SeV particles, as was observed for IAV (17). These data demonstrated that TMPRSS2 proteolytically activated the SeV F protein intracellularly during the process of SeV assembly. Therefore, the mechanism for SeV and IAV activation by TMPRSS2 is different from that for the SARS coronavirus, which is activated at the entry step after receptor binding (11).

The F proteins of HMPV, SeV, HPIV1, and HPIV4 (both HPIV4a and HPIV4b) and the HA protein of IAV (H1 subtype) possess serine and glutamine residues at the P2 and P3 positions, respectively (Table 1). These residues are relatively conserved among respiratory viruses (Table 1). An arginine or a lysine residue at P1 is mandatory for serine protease substrates, while the residues at P2 and P3 are much more flexible than the P1 residue, although they may also modulate the specificity of the protease substrate (18, 19). By site-directed mutagenesis of pSeV-RFP, five predicted amino acid substitutions (Q114A, Q114S, Q114V, S115R, and S115V) were individually introduced into the F protein of recombinant SeV. The mutated hexanucleotide sequences, which correspond to amino acid residues at positions 114 and 115 of the Q114A, Q114S, Q114V, S115R, and S115V mutants, were GCCTCG, AGCTCG, GTGTCG, ATCCGC, and ATCGTG, respectively (mutated nucleotides are underlined). Infectious SeV mutants were generated by using a reverse-genetics technique (15). The replication capacities of the mutant SeVs were analyzed using TMPRSS2-expressing Huh7 cells (Huh7/TMPRSS2-18 and Huh7/TMPRSS2m-4 cell lines) (M. Esumi et al., submitted for publication). Huh7/TMPRSS2-18 cells constitutively express an intact and active form of TMPRSS2, while Huh7/TMPRSS2m-4 cells constitutively express an enzymatically inactive mutant form of TMPRSS2 (TMPRSS2m) with an S441A mutation (Esumi et al., submitted). In Huh7/TMPRSS2m-4 cells, all of the SeVs, including SeV-RFP(wt), spread slowly, whereas in Huh7/TMPRSS2-18 cells, all of the viruses spread much more efficiently (Fig. 2A and B). However, in Huh7/TMPRSS2-18 cells, the growth of the mutant SeV with S115R (SeV-RFP/S115R) was severely deteriorated, and the infectious-virus production was more than 1,000 times lower than that of SeV-RFP(wt) (Fig. 2A and B). The other four mutants (SeV-RFP/Q114S, -RFP/Q114A, -RFP/Q114V, and -RFP/S115V) also showed impaired replication capacities that were reduced by ~10-fold (Fig. 2B). However, pulse-chase labeling followed by immunoprecipitation and SDS-PAGE showed little, if any, effects of the mutations on the cleavage of the F proteins of the recombinant SeVs in Huh7/TMPRSS2-18 cells (Fig. 2C).

Human bronchial epithelial Calu-3 cells and intestinal epithelial Caco-2 cells have an intrinsic ability to proteolytically activate IAV using endogenously expressed proteases (20–22). In Calu-3 cells, TMPRSS2 and matriptase were shown to contribute to IAV HA cleavage (6, 21). In Caco-2 cells, TMPRSS2 and TMPRSS4 are

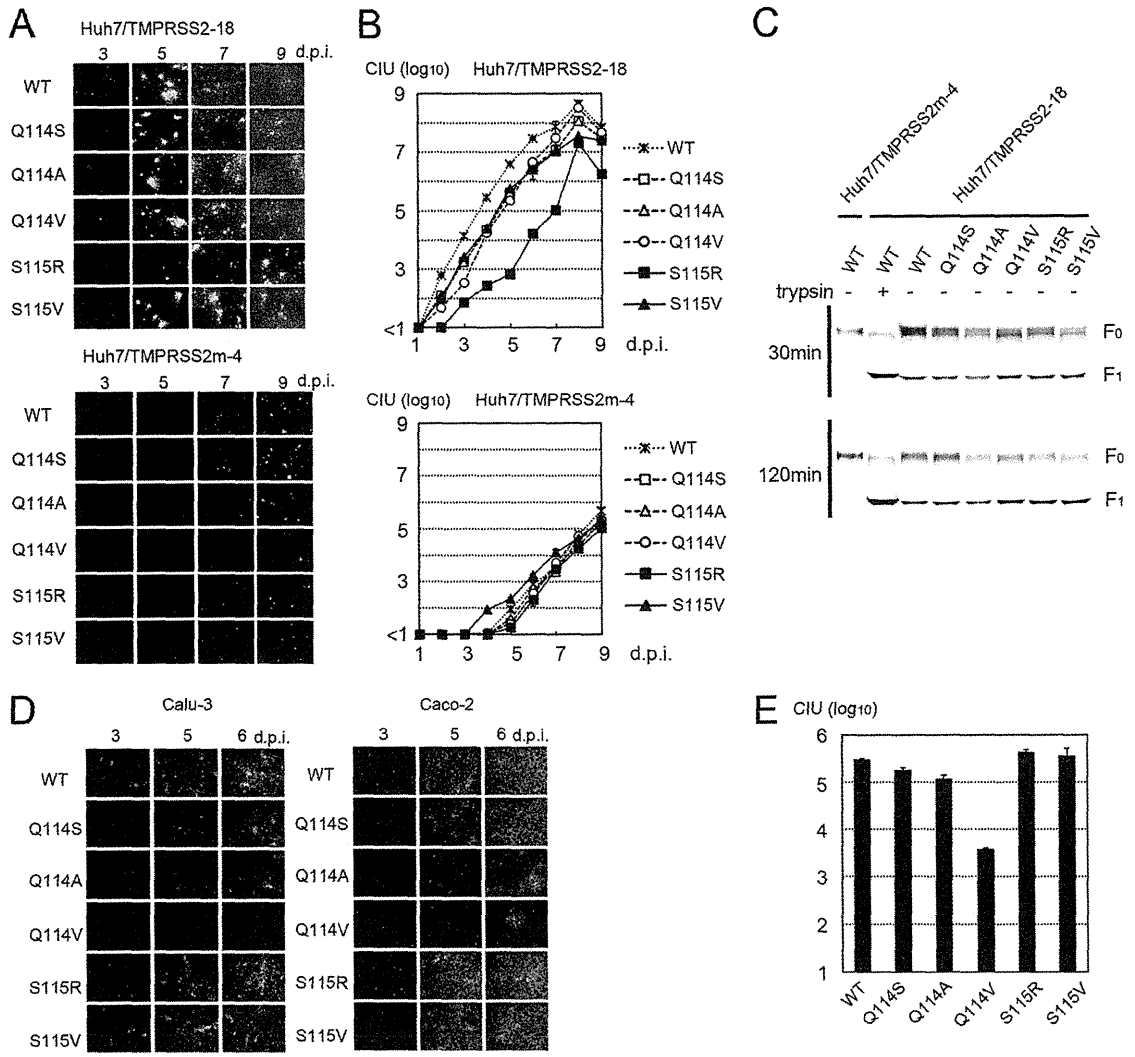

FIG 2 Analyses of recombinant SeV-RFP strains with mutations at P2 and P3 of the F protein. (A) Detection of wt- and mutant-SeV-RFP-infected cells. Monolayers of Huh7/TMPRSS2-18 and Huh7/TMPRSS2m-4 cells were infected with wt and mutant SeV-RFPs at an MOI of 0.01, cultured in the absence of trypsin, and observed daily using a fluorescence microscope. Data at 3, 5, 7, and 9 days postinfection are shown. (B) Replication kinetics of wt and mutant SeV-RFPs in Huh7/TMPRSS2-18 and Huh7/TMPRSS2m-4 cells. Cells were infected with wt and mutant SeV-RFPs at an MOI of 0.01, cultured in the absence of trypsin, and examined for their virus titers (CIU) daily. (C) Pulse-chase labeling, immunoprecipitation, and SDS-PAGE for detection of SeV F proteins. Huh7/TMPRSS2-18 and Huh7/TMPRSS2m-4 cells infected with wt or mutant SeV-RFP were pulse-labeled with [^{35}S]methionine for 15 min, cultured (chased) in normal medium for 30 or 120 min, and subjected to immunoprecipitation and SDS-PAGE for detection of the F proteins. (D) Detection of wt- and mutant-SeV-RFP-infected cells. Monolayers of Calu-3 and Caco-2 cells were infected with wt and mutant SeV-RFPs at an MOI of 0.001, cultured in the absence of trypsin, and observed daily using a fluorescence microscope. Data at 3, 5, and 6 days postinfection are shown. (E) Virus production in Calu-3 cells. Calu-3 cells were infected with wt and mutant SeV-RFPs at an MOI of 0.001 and examined for their virus titers (CIU) at 5 days postinfection.

responsible for activation of the IAV HA (22). Calu-3 and Caco-2 cells were infected with SeV-RFP(wt) and mutant SeVs. Both cell lines supported SeV-RFP(wt) multiplication well (Fig. 2D), similar to what occurred with IAV (20–22). All of the mutant SeVs also underwent multiple rounds of infection in both cell lines. However, unlike with Huh7/TMPRSS2-18 cells, the propagation of SeV-RFP/Q114V was severely deteriorated in these cell lines, whereas SeV-RFP/S115R spread well in these cell lines (Fig. 2D and E). Although not as dramatically, the other two mutants with mutations at P3 (SeV-RFP/Q114S and -RFP/Q114A) also spread less efficiently than SeV-RFP(wt) in these cell lines (Fig. 2D and E). Thus, the effects of each mutation observed in Calu-3 and Caco-2 cells were different from those observed in TMPRSS2-expressing Huh7 cells. Since Calu-3 and Caco-2 cells have more than one protease contributing to IAV HA activation, the SeV F protein may be activated mainly by proteases other than TMPRSS2 in these cells. Nevertheless, the glutamine residue at P3 was shown to be important for SeV multiplication in bronchial and intestinal epithelial cells.

The present study has demonstrated the importance of the P2 serine and P3 glutamine residues for SeV replication, but the roles of these residues remain unclear. Although our data showed little, if any, effects of the mutations on F protein cleavage by TMPRSS2, these residues may modulate the protease's specificity or sensitiv-

ity for the F protein. Many proteases have been shown to activate respiratory viruses. Trypsin is commonly used for the propagation of IAV, HMPV, SeV, HPIVs, and coronaviruses in cultured cells. Mini-plasmin found in bronchial epithelia (23), tryptase Clara from rat lungs (24, 25), mast cell tryptase from porcine lungs (26), and factor Xa from chicken allantoic fluid (26) were shown to proteolytically activate IAV and SeV. Plasmin also activates IAV through unique mechanisms by which plasminogen is captured by the neuraminidase surface glycoprotein or host cell annexin II is incorporated into virions (27–29). Recent studies have added a new class of proteases, transmembrane serine proteases (TTSPs), to the list of IAV- or SeV-activating proteases (2). TMPRSS2, HAT (TMPRSS11D), and TMPRSS4 were shown to activate seasonal IAV strains (3, 4, 21, 22). However, it remains totally unknown which proteases contribute mainly to respiratory virus pathogenesis. Although multiple proteases may contribute to the virus' spread *in vivo*, membrane-anchored proteases have an advantage for processing target substrates at a specific location with a minimum concentration (30, 31). Indeed, our previous study demonstrated that a marginal level of TMPRSS2 expression was sufficient for intracellular cleavage of the IAV HA and HMPV F proteins (7). To date, the biological and physiological functions of TMPRSS2 have been poorly elucidated. Although a previous study suggested that TMPRSS2 regulates the Na^+ current (32), the physiological importance of this is uncertain, because TMPRSS2 knockout mice showed no developmental, physiological, or pathological changes from wild-type mice (33). A final conclusion awaits *in vivo* analyses for the contribution of TMPRSS2 to viral pathogenesis. However, the accumulated evidence has revealed that TMPRSS2 acts as an activating protease for a broad range of respiratory viruses.

ACKNOWLEDGMENTS

We thank N. Ito and M. Sugiyama for providing the BHK/T7-9 cells. We also thank all the members of Department of Virology 3, NIID, Japan, for technical support.

This work was supported by grants from the Ministry of Education, Culture, Sports, Science and Technology and the Ministry of Health, Labor and Welfare of Japan and by a grant from The Takeda Science Foundation.

REFERENCES

1. **Kido H, Okumura Y, Takahashi E, Pan HY, Wang S, Chida J, Le TQ, Yano M.** 2008. Host envelope glycoprotein processing proteases are indispensable for entry into human cells by seasonal and highly pathogenic avian influenza viruses. J. Mol. Genet. Med. 3:167–175.
2. **Choi SY, Bertram S, Glowacka I, Park YW, Pohlmann S.** 2009. Type II transmembrane serine proteases in cancer and viral infections. Trends Mol. Med. 15:303–312.
3. **Chaipan C, Kobasa D, Bertram S, Glowacka I, Steffen I, Tsegaye TS, Takeda M, Bugge TH, Kim S, Park Y, Marzi A, Pohlmann S.** 2009. Proteolytic activation of the 1918 influenza virus hemagglutinin. J. Virol. 83:3200–3211.
4. **Bottcher E, Matrosovich T, Beyerle M, Klenk HD, Garten W, Matrosovich M.** 2006. Proteolytic activation of influenza viruses by serine proteases TMPRSS2 and HAT from human airway epithelium. J. Virol. 80: 9896–9898.
5. **Hamilton BS, Gludish DW, Whittaker GR.** 2012. Cleavage activation of the human-adapted influenza virus subtypes by matriptase reveals both subtype and strain specificities. J. Virol. 86:10579–10586.
6. **Beaulieu A, Gravel E, Cloutier A, Marois I, Colombo E, Desilets A, Verreault C, Leduc R, Marsault E, Richter MV.** 2013. Matriptase proteolytically activates influenza virus and promotes multicycle replication in the human airway epithelium. J. Virol. 87:4237–4251.
7. **Shirogane Y, Takeda M, Iwasaki M, Ishiguro N, Takeuchi H, Nakatsu Y, Tahara M, Kikuta H, Yanagi Y.** 2008. Efficient multiplication of human metapneumovirus in Vero cells expressing the transmembrane serine protease TMPRSS2. J. Virol. 82:8942–8946.
8. **Bertram S, Glowacka I, Muller MA, Lavender H, Gnirss K, Nehlmeier I, Niemeyer D, He Y, Simmons G, Drosten C, Soilleux EJ, Jahn O, Steffen I, Pohlmann S.** 2011. Cleavage and activation of the severe acute respiratory syndrome coronavirus spike protein by human airway trypsin-like protease. J. Virol. 85:13363–13372.
9. **Glowacka I, Bertram S, Muller MA, Allen P, Soilleux E, Pfefferle S, Steffen I, Tsegaye TS, He Y, Gnirss K, Niemeyer D, Schneider H, Drosten C, Pohlmann S.** 2011. Evidence that TMPRSS2 activates the severe acute respiratory syndrome coronavirus spike protein for membrane fusion and reduces viral control by the humoral immune response. J. Virol. 85:4122–4134.
10. **Shulla A, Heald-Sargent T, Subramanya G, Zhao J, Perlman S, Gallagher T.** 2011. A transmembrane serine protease is linked to the severe acute respiratory syndrome coronavirus receptor and activates virus entry. J. Virol. 85:873–882.
11. **Matsuyama S, Nagata N, Shirato K, Kawase M, Takeda M, Taguchi F.** 2010. Efficient activation of the severe acute respiratory syndrome coronavirus spike protein by the transmembrane protease TMPRSS2. J. Virol. 84:12658–12664.
12. **Kawase M, Shirato K, van der Hoek L, Taguchi F, Matsuyama S.** 2012. Simultaneous treatment of human bronchial epithelial cells with serine and cysteine protease inhibitors prevents severe acute respiratory syndrome coronavirus entry. J. Virol. 86:6537–6545.
13. **Gierer S, Bertram S, Kaup F, Wrensch F, Heurich A, Kramer-Kuhl A, Welsch K, Winkler M, Meyer B, Drosten C, Dittmer U, von Hahn T, Simmons G, Hofmann H, Pohlmann S.** 2013. The spike protein of the emerging betacoronavirus EMC uses a novel coronavirus receptor for entry, can be activated by TMPRSS2 and is targeted by neutralizing antibodies. J. Virol. 87:5502–5511.
14. **Karron RA, Collins PL.** 2007. Parainfluenza viruses, p 1497–1526. *In* Knipe DM, Howley PM, Griffin DE, Lamb RA, Martin MA, Roizman B, Straus SE (ed), Fields virology, 5th ed. Lippincott Williams & Wilkins, Philadelphia, PA.
15. **Kato A, Sakai Y, Shioda T, Kondo T, Nakanishi M, Nagai Y.** 1996. Initiation of Sendai virus multiplication from transfected cDNA or RNA with negative or positive sense. Genes Cells 1:569–579.
16. **Hasan MK, Kato A, Shioda T, Sakai Y, Yu D, Nagai Y.** 1997. Creation of an infectious recombinant Sendai virus expressing the firefly luciferase gene from the 3′ proximal first locus. J. Gen. Virol. 78(Part 11):2813–2820.
17. **Bottcher-Friebertshauser E, Freuer C, Sielaff F, Schmidt S, Eickmann M, Uhlendorff J, Steinmetzer T, Klenk HD, Garten W.** 2010. Cleavage of influenza virus hemagglutinin by airway proteases TMPRSS2 and HAT differs in subcellular localization and susceptibility to protease inhibitors. J. Virol. 84:5605–5614.
18. **Gosalia DN, Salisbury CM, Ellman JA, Diamond SL.** 2005. High throughput substrate specificity profiling of serine and cysteine proteases using solution-phase fluorogenic peptide microarrays. Mol. Cell. Proteomics 4:626–636.
19. **Gosalia DN, Salisbury CM, Maly DJ, Ellman JA, Diamond SL.** 2005. Profiling serine protease substrate specificity with solution phase fluorogenic peptide microarrays. Proteomics 5:1292–1298.
20. **Zhirnov O, Klenk HD.** 2003. Human influenza A viruses are proteolytically activated and do not induce apoptosis in CACO-2 cells. Virology 313:198–212.
21. **Bottcher-Friebertshauser E, Stein DA, Klenk HD, Garten W.** 2011. Inhibition of influenza virus infection in human airway cell cultures by an antisense peptide-conjugated morpholino oligomer targeting the hemagglutinin-activating protease TMPRSS2. J. Virol. 85:1554–1562.
22. **Bertram S, Glowacka I, Blazejewska P, Soilleux E, Allen P, Danisch S, Steffen I, Choi SY, Park Y, Schneider H, Schughart K, Pohlmann S.** 2010. TMPRSS2 and TMPRSS4 facilitate trypsin-independent spread of influenza virus in Caco-2 cells. J. Virol. 84:10016–10025.
23. **Murakami M, Towatari T, Ohuchi M, Shiota M, Akao M, Okumura Y, Parry MA, Kido H.** 2001. Mini-plasmin found in the epithelial cells of bronchioles triggers infection by broad-spectrum influenza A viruses and Sendai virus. Eur. J. Biochem. 268:2847–2855.
24. **Kido H, Yokogoshi Y, Sakai K, Tashiro M, Kishino Y, Fukutomi A, Katunuma N.** 1992. Isolation and characterization of a novel trypsin-like protease found in rat bronchiolar epithelial Clara cells. A possible activator of the viral fusion glycoprotein. J. Biol. Chem. 267:13573–13579.

25. **Tashiro M, Yokogoshi Y, Tobita K, Seto JT, Rott R, Kido H.** 1992. Tryptase Clara, an activating protease for Sendai virus in rat lungs, is involved in pneumopathogenicity. J. Virol. **66**:7211–7216.
26. **Chen Y, Shiota M, Ohuchi M, Towatari T, Tashiro J, Murakami M, Yano M, Yang B, Kido H.** 2000. Mast cell tryptase from pig lungs triggers infection by pneumotropic Sendai and influenza A viruses. Purification and characterization. Eur. J. Biochem. **267**:3189–3197.
27. **Goto H, Kawaoka Y.** 1998. A novel mechanism for the acquisition of virulence by a human influenza A virus. Proc. Natl. Acad. Sci. U. S. A. **95**:10224–10228.
28. **Lazarowitz SG, Goldberg AR, Choppin PW.** 1973. Proteolytic cleavage by plasmin of the HA polypeptide of influenza virus: host cell activation of serum plasminogen. Virology **56**:172–180.
29. **LeBouder F, Morello E, Rimmelzwaan GF, Bosse F, Pechoux C, Delmas B, Riteau B.** 2008. Annexin II incorporated into influenza virus particles supports virus replication by converting plasminogen into plasmin. J. Virol. **82**:6820–6828.
30. **Hooper JD, Clements JA, Quigley JP, Antalis TM.** 2001. Type II transmembrane serine proteases. Insights into an emerging class of cell surface proteolytic enzymes. J. Biol. Chem. **276**:857–860.
31. **Antalis TM, Buzza MS, Hodge KM, Hooper JD, Netzel-Arnett S.** 2010. The cutting edge: membrane-anchored serine protease activities in the pericellular microenvironment. Biochem. J. **428**:325–346.
32. **Donaldson SH, Hirsh A, Li DC, Holloway G, Chao J, Boucher RC, Gabriel SE.** 2002. Regulation of the epithelial sodium channel by serine proteases in human airways. J. Biol. Chem. **277**:8338–8345.
33. **Kim TS, Heinlein C, Hackman RC, Nelson PS.** 2006. Phenotypic analysis of mice lacking the Tmprss2-encoded protease. Mol. Cell. Biol. **26**:965–975.

Journal of Vaccines & Immunization

Nagata S et al., J Vaccines Immun 2013, 1(2): 13-21
http://dx.doi.org/10.14312/2053-1273.2013-3

NobleResearch

Original research

Open Access

Comparison of the live attenuated mumps vaccine (Miyahara strain) with its preattenuated parental strain

Nagata S[1], Maedera T[1], Nagata N[2], Kidokoro M[1], Takeuchi K[3], Kuranaga M[4], Takedaa M[1] and Kato A[1*]

[1]Department of Virology III, National Institute of Infectious Diseases, Musashi-Murayama, 208-0011, Japan
[2]Department of Pathology, National Institute of Infectious Diseases, Musashi-Murayama, 208-0011, Japan
[3]Department of Infection Biology, Division of Biomedical Science, Faculty of Medicine, University of Tsukuba, Tsukuba, 305-0006, Japan
[4]The Chemo-Sero-Therapeutic Research Institute (KAKETSUKEN), Kumamoto, 860-0083, Japan

Abstract

Live attenuated mumps vaccines have been developed by passaging the field isolates in cells that differ from the natural host. To study mumps viral (MuV) attenuation at the genomic level, we compared a live attenuated mumps vaccine (Miyahara strain) to its preattenuated parental strain. These two strains exhibited several phenotypic differences. The parental strain grew faster, reached a higher titer, and formed larger plaques and syncytia in Vero cells compared to the vaccine strain. In addition, intracranial injection of parental strain in neonatal rats resulted in greater ventricular enlargement than that caused by the vaccine strain. Four nucleotide changes leading to amino acid substitutions were found between the two viral genomes. One change is present in the N and L genes, respectively, and two in the F gene. The fusogenic activity of the cloned parental F gene evaluated by a cell-cell fusion assay was weaker than that of the vaccine F gene, and did not correspond to the activity caused by the living parental and vaccine strains. The transcriptional activities of N and L proteins were monitored by a CAT minigenome assay. Cloned parental N gene produced almost the same CAT activity as vaccine N, and cloned parental L gene produced significantly higher CAT activity than vaccine L. Thus among four nucleotide changes, the three occurring in N and F were not found to relate to the viral outcome, but we confirmed that at least one change in the L protein was involved in the growth phenotype of parental MuV.

Keywords: attenuation; fusion; mumps virus; neurovirulence; replication; vaccine; Miyahara strain

Introduction

Mumps is an acute, contagious vaccine-preventable disease caused by the mumps virus (MuV). A mumps epidemic occurs every 3 to 5 years in unvaccinated populations, and humans are the only natural host for MuV infection. MuV is transmitted by the respiratory route and replicates primarily in the nasal epithelium, leading to viremia, and it triggers secondary viral replication [1]. Up to 30% of MuV infections are asymptomatic or show only nonspecific respiratory symptoms. In 70% to 90% of symptomatic infections, MuV invasion of glandular epithelium results in mumps parotitis. MuV enters the cerebrospinal fluid (CSF) during the viremia. CSF pleocytosis leads to a form of aseptic meningitis that occurs in about 10% of mumps cases. More serious complications, such as deafness and encephalitis, occur at a low frequency [1].

MuV belongs to the genus *Rubulavirus* of the family *Paramyxoviridae* and has a negative-strand nonsegmented RNA genome of 15,384 bases with seven genes encoding eight proteins: the nucleocapsid (N), V, phospho (P), matrix (M), fusion (F), small hydrophobic (SH), hemagglutinin-neuraminidase (HN), and large (L) proteins. The N, P, and L proteins participate in viral replication and, together with the genomic RNA, form the ribonucleocapsid (RNP). In the virion, RNP is surrounded by a host-derived membrane undercoated by the M protein. The HN and F

***Corresponding author:** Atsushi Kato, Division of Radiological Protection and Biology, National Institute of Infectious Diseases, 1-23-1 Toyama, Shinjuku-ku, Tokyo, 162-8640, Japan, Tel.: 81 3 5285 1111, ext. 2421; Fax: 81 3 5285 1194; E-mail: akato@niid.go.jp

Received 22 April 2013 *Revised* 15 July 2013 *Accepted* 22 July 2013 *Published* 29 July 2013

Citation: Nagata S, Maedera T, Nagata N, Kidokoro M, Takeuchi K, Kuranaga M, Takedaa M, Kato A (2013) Comparison of the live attenuated mumps vaccine (Miyahara Strain) with its preattenuated parental strain. J Vaccines Immun 1: 13-21. doi:10.14312/2053-1273.2013-3

proteins projected onto the virion surface are responsible for cell binding and the entry of MuV. The functions of V and SH are less well understood [2–5]. The SH gene sequence is variable and is therefore used as the basis of MuV genotyping [6–8].

Live attenuated MuV vaccines have been developed by adapting the virus for different species of host or for different conditions of temperature, after repeated trial and error. The first vaccine, Jeryl Lynn strain, was introduced into the USA in 1967 and contributed to a dramatic reduction in mumps infection rates. To date, more than 10 vaccines have been produced. Some vaccines were found to retain a limited pathogenicity [9–11], and some tend to lose immunogenicity because of over-attenuation [12]. Five vaccines were developed in Japan (Urabe [13], Hoshino [14], Torii, Miyahara and NK-M46), and they were found to cause aseptic meningitis, although much less frequently than the natural infection rate [15, 16]. The virulence of MuV has recently been studied using the reverse genetic techniques established for Jeryl Lynn strain cDNA [17]. The genetic basis for attenuation has been vigorously studied [18–23], but a common genetic factor for MuV attenuation has not yet been identified.

In this study, we compared a Japanese mumps vaccine, Miyahara strain, with its parental strain in the preattenuated position to investigate the molecular basis of attenuation. The parental strain apparently has a different phenotype. The full genome sequences of the parental strain and the vaccine revealed four nucleotide substitutions. Those changes accompany the amino acid substitution, and one amino acid change occurring in the L protein was linked to replication capacity *in vitro*.

Materials and methods

Viruses

The MuV Miyahara isolate was originally obtained from a mumps patient in 1970 in Japan. A passage history of the Miyahara strain is indicated in Figure 1. The Miyahara field isolate had been lost, but the strain that locates on the preadapted position of chicken embryo fibroblasts (CE) passages (exact position was not known) was retrieved from the freezer of the National Institute of Infectious Diseases, Japan and used in this study as a parental strain with the approval of the Kaketsuken (the Chemo-Sero-Therapeutic Research Institute, Kumamoto, Japan). We purchased the live attenuated Miyahara MuV vaccine (lot 305) from the Chemo-Sero-Therapeutic Research Institute. Wild-type MuVodate-1 [24,25] and 02-49 were kindly provided by Dr. H. Saito (Akita Prefectural Institute of Public Health, Akita, Japan) and Dr. Y. Matsui (Niigata Prefectural Institute of Public Health and Environmental Science, Niigata, Japan), respectively. In all virus stocks used in this study, defective interfering particles that might influence the results were not found.

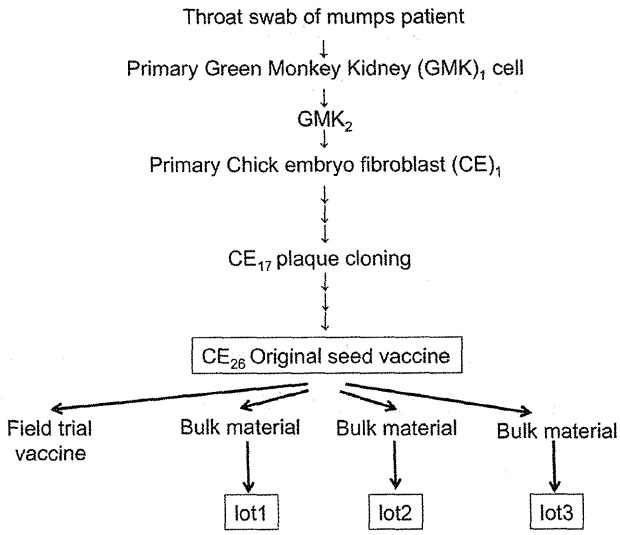

Figure 1 Passage history of the MuV Miyahara strain. MuV originally isolated from a throat swab of a 4-year old female mumps patient in primary green monkey kidney cells is shown as GMK_1. Another passage in the same GMK cells is shown as GMK_2. Passages in the primary cell culture of chick embryo fibroblasts are shown as CE. At the 17th passage of CE (CE_{17}), MuV was plaque purified. The test lot produced from CE_{26} was administered as the field trial vaccine. CE_{26} was licensed as the original seed for a live attenuated mumps vaccine, the Miyahara strain, in 1985 in Japan. The exact position of the Miyahara parental strain used in this study is not mapped due to the loss of records. Three bulk materials (lots 1, 2, and 3) have been produced, and the vaccine (lot 305) used in this study was produced from bulk lot 3.

Cell cultures and virus infection

Vero cells were grown in minimal essential medium (MEM) supplemented with 5% (v/v) bovine serum (BS) and inoculated with parental or vaccine strains at a multiplicity of infection (m.o.i.) of 0.01 cell infection unit (CIU)/cell unless otherwise noted. BHK-T7 cells [26] were kindly supplied by Dr. N. Ito (Gifu University, Gifu, Japan), and were maintained in Glasgow-MEM (Life Technologies Japan, Tokyo) containing 5% fetal BS.

For the growth kinetics study of parental and vaccine strains, 0.1 mL of culture supernatant was harvested daily until 5 days post-infection. The virus titer was then measured at least five times in each sample. MuV strains were titrated using Vero cells. Briefly, a diluted series of MuV was inoculated onto confluent cells in a 12-well plate after the removal of medium. After adsorption for 1 h, 1 mL of medium was added to each well. Thirty-six hours later, infected cells were treated with rabbit anti-MuV hyperimmune serum followed by fluorescein isothiocyanate (FITC)-conjugated anti-rabbit immunoglobulin G. FITC-positive cells were measured, and the virus titer (CIU/ml) was calibrated.

For plaque formation, MuV was inoculated onto confluent Vero cells in a 6-well plate. After adsorption for 1 h, 1.0% (w/v) agarose in MEM containing 0.5% BS was overlaid on the cell culture and incubated at 37°C for 8 days. An agarose in MEM containing 0.01% (w/v) Neutral Red solution